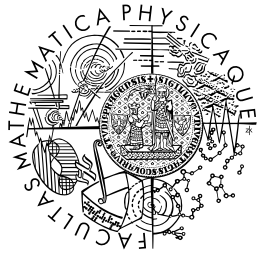

FACULTY
OF MATHEMATICS
AND PHYSICS
Charles University

BACHELOR THESIS

Oldřich Sedlák

Quantum Thermodynamics

Department of Macromolecular Physics

Supervisor of the bachelor thesis: RNDr. Viktor Holubec, Ph.D.
Study programme: Physics
Study branch: General Physics

Prague 2018

I declare that I carried out this bachelor thesis independently, and only with the cited sources, literature and other professional sources.

I understand that my work relates to the rights and obligations under the Act No.121/2000 Sb., the Copyright Act, as amended, in particular, the fact that the Charles University has the right to conclude a license agreement on the use of this work as a school work pursuant to Section 60 subsection 1 of the Copyright Act.

In Prague date 19.7.2018 signature of the author

Title: Quantum Thermodynamics

Author: Oldřich Sedlák

Department: Department of Macromolecular Physics

Supervisor: RNDr. Viktor Holubec, Ph.D., Department of Macromolecular Physics

Abstract:

Quantum coherence is being viewed as a possible resource that could improve the performance of quantum technologies. This thesis analyzes a quantum heat engine model inspired by Dorfman et al. (PNAS vol. 110 no. 8) while using a standard Markovian quantum optical master equation in the Lindblad form. Steady-state coherence arises from the degeneracy of the two upper energy levels and its effects become significant for near-perfect alignment of the associated transition dipole moments. For the maximum alignment, the steady-state current becomes highly dependent on the relative phase and exhibits quantum interference. The performed numerical calculations show some promise of possible enhancement of the current above the classical limit.

Keywords: quantum coherence, quantum thermodynamics, open quantum system

I would like to express my appreciation to my supervisor RNDr. Viktor Holubec, Ph.D. for going above and beyond in keeping me focused but also for allowing me to delve into parts I found most interesting. I am grateful for his permanent support and dedication in helping me complete this thesis.

Contents

Introduction

Quantum coherence is being viewed as a possible resource that could improve the performance of quantum technologies and attempts are being made to precisely quantify its usefulness [1]. A discovery that sparked research interest in quantum effects in biology was the observation of long-lived coherence in natural light-harvesting systems [2]. Without a doubt, the study of the various quantum effects [3, 4, 5, 6] present in photosynthetic systems could be highly beneficial to the development of new enhanced artificial solar cells and nanotechnologies. For example, in the first phase of photosynthesis antennae complexes harvest solar energy which is used for charge separation carried out by the photosynthetic reaction centre. The quantum efficiency of this process can under certain conditions exceed 95 % [7]. In other words, each absorbed photon almost certainly reaches the reaction centre and drives the separation of charge.

Inspired by the observed coherence phenomena [2], Dorfman et al. have proposed a simple quantum heat engine (QHE) model [8] based on a pair of tightly coupled chlorophylls at the heart of the reaction centre. In their model, coherence between two populations representing this special pair can boost the classical photocurrent by 27 %. While theoretical results look promising, they (Dorfman et al.) also comment, however, that the quantum coherence effects observed in photosynthetic experiments are studied with coherent laser radiation that might affect the natural conditions of excitation by solar incoherent light.

This thesis further explores the effects of coherence on a very similar model. The first two chapters serve as an introduction of the used Markovian quantum optical master equation, including its application to a simple system. The third chapter introduces the model of the QHE, the equations of motion and the physical quantities used for the analysis of the engine. Finally, the last chapter analyzes the effects of coherence, focusing mainly on the steady-state current in the QHE.

1. Theoretical background

This chapter consists of two sections. First, we briefly review the concept of an open quantum system and in the second section, we take a look at the necessary assumptions required for the validity of our Markovian description of the dynamics.

1.1 Introduction to open quantum systems

The main mathematical distinction between an idealized closed system and an open quantum system is that the Hamiltonian dynamics of closed systems is reversible and can be represented by unitary transformations. This is generally not the case for open quantum systems where we consider the interactions with the environment. The resulting irreversible dynamics is then associated with the production of entropy. An open quantum system is, therefore, a system S interacting with another external system B which we generally call the *environment*. If an environment has an infinite number of degrees of freedom it is called a *reservoir* and if a reservoir is in a thermal equilibrium state we call it a *heat bath* or simply a *bath* [9].

The introduction of the environment B to the system S expands the Hilbert space,

$$\mathcal{H} = \mathcal{H}_S \otimes \mathcal{H}_B.$$

Consequently, the operator $\hat{O}$ previously acting in the Hilbert space $\mathcal{H}_S$ needs to be expanded over the combined Hilbert space $\mathcal{H}$ with the identity operator $\hat{I}_B$ of the environment to $\hat{O} \otimes \hat{I}_B$. The expectation value is then obtained as:

$$\langle O \rangle(t) = \mathrm{tr}\{(\hat{O} \otimes \hat{I}_B)\hat{\rho}(t)\} = \mathrm{tr}_S\{\hat{O}\hat{\rho}_S(t)\},$$

where $\hat{\rho}$ is the density matrix of the combined system $S + B$ and $\hat{\rho}_S$ is the *reduced density matrix* describing the open system,

$$\hat{\rho}_S(t) = \mathrm{tr}_B\{\hat{\rho}(t)\}.$$

The dynamics of the open system follows from the dynamics of the combined system which is governed by its Hamiltonian $\hat{H}$ and the Schrödinger equation. This Hamiltonian consists of the self-Hamiltonians of the open system and the environment, $\hat{H}_S$ and $\hat{H}_B$, and the Hamiltonian $\hat{H}_I$ describing the interaction between the two systems [9],

$$\hat{H} = \hat{H}_S \otimes \hat{I}_B + \hat{I}_S \otimes \hat{H}_B + \hat{H}_I.$$

The evolution from time t_0 to time t can be expressed with the evolution operator $\hat{U}(t, t_0)$ [10],

$$\hat{\rho}(t) = \hat{U}(t, t_0)\hat{\rho}(t_0)\hat{U}^\dagger(t, t_0).$$

In the case of a time-independent Hamiltonian $\hat{H}$, the operator $\hat{U}(t, t_0)$ has the well-known form:

$$\hat{U}(t, t_0) = \exp\left[-\frac{i}{\hbar}\hat{H}(t - t_0)\right],$$

where $\hbar$ is the reduced Planck constant.

1.2 Markovian evolution and Lindblad form

In general, the evolution of the density matrix $\hat{\rho}_S$ can depend on its history (earlier states of the open system) because changes in the open system can be remembered by the environment which can, in turn, affect the open system at a later time.

In some situations, however, these memory effects can be neglected. In that case, it is possible to form an approximate description where the conditional evolution to future states, given the present state of the open system $\hat{\rho}_S(t)$, does not depend on any past states but only on the present state. We call this in the context of stochastic processes the Markovian property.

Let us assume that the memory in the environment (information in the form of correlations) caused by the changes in the open system that we want to follow is lost after time Δt. This can happen through strong effects of decoherence. The time Δt then sets the scale of this so-called time coarse-graining, i.e. the shortest period of time over which the behavior of the open system can be determined [11, 12]. It follows that we must also assume that the open system changes appreciably over a typical timescale τ_S much larger than this time Δt:

$$\tau_S \gg \Delta t.$$

Furthermore, when deriving this Markovian master equation for $\hat{\rho}_S$, we would like to preserve the properties of the general Kraus representation [13] of the evolution. These properties include linearity, hermicity preservation, trace preservation and complete positivity. For example, this can be done through the process of time coarse-graining described above along with the assumption of weak interaction (to second order) between the open system and the environment [11, 12]. The resulting equation is then in the Lindblad form which is the most general Markovian master equation with these properties [9].

If we restrict ourselves to a time-independent Hamiltonian $\hat{H}_S$ and the interaction Hamiltonian in the form $\hat{H}_I = \hat{A} \otimes \hat{B}$, the Lindblad form can be expressed with the use of eigenoperators of the open system,

$$\hat{A}_\omega = \sum_{\hbar\omega = \epsilon' - \epsilon} |\epsilon\rangle \langle\epsilon| \hat{A} |\epsilon'\rangle \langle\epsilon'| ,$$

where the sum runs over all energy eigenvalues ϵ' and ϵ of $\hat{H}_S$ such that their difference corresponds to the transition frequency $\omega = (\epsilon' - \epsilon)/\hbar$. The master equation in the Lindblad form expressed for the reduced density matrix in the interaction picture $\hat{\rho}_{S_I}$ reads:

$$\frac{d}{dt}\hat{\rho}_{S_I}(t) = -\frac{i}{\hbar}[\hat{H}_U(\Delta t), \hat{\rho}_{S_I}(t)] + \sum_{\omega,\omega'} \gamma_{\omega\omega'}(\Delta t)\left(\hat{A}_\omega \hat{\rho}_{S_I}(t) \hat{A}^\dagger_{\omega'} - \frac{1}{2}\left\{\hat{A}^\dagger_{\omega'}\hat{A}_\omega, \hat{\rho}_{S_I}(t)\right\}\right), \quad (1.1)$$

where it is required that $\hat{H}_U$ is hermitian and the rates $\gamma_{\omega\omega'}(\Delta t)$ form a positive matrix [12].

The first term in (1.1) accounts for the unitary part of the evolution of the open system while the rest serves to describe the non-unitary dynamics. Note that the non-unitary part is summed over two sets of possible transition frequencies (ω and ω') and that there are terms depending on the coarse-graining parameter Δt.

2. Quantum optical master equation

Microscopic and phenomenological derivations of Markovian master equations often rely on further assumptions and the resulting master equation may not come out in the Lindblad form. This can lead to pathological behaviour such as violation of positivity [14]. For our model, we use a standard quantum optical master equation (QOME) whose derivation can be found in many textbooks, such as *The Theory of Open Quantum Systems* by Breuer and Petruccione [9]. In our derivation, the Lindblad form is ensured with the use of the rotating wave approximation (RWA).

2.1 Microscopic assumptions and derivation

Our quantum optical master equation assumes the following Hamiltonian:

$$\hat{H} = \sum_{i}^{N} \hbar\omega_i \left|i\right\rangle \left\langle i\right| + \sum_{\vec{k}} \sum_{\lambda=1,2} \hbar\omega_k \hat{a}_\lambda^\dagger(\vec{k})\hat{a}_\lambda(\vec{k}) - e\hat{\vec{D}} \cdot \hat{\vec{E}}. \tag{2.1}$$

- The open system has a discrete energy spectrum with N well-spaced energy levels,

$$\hat{H}_S = \sum_{i}^{N} \hbar\omega_i \left|i\right\rangle \left\langle i\right|, \tag{2.2}$$

  where energy eigenstates $|i\rangle$ have eigenvalues E_i proportional to the angular frequencies ω_i ($E_i = \hbar\omega_i$).

- The heat bath is represented by a quantized electromagnetic field that is in a thermodynamic equilibrium at temperature T, i.e. it is an ideal black body radiation,

$$\hat{H}_B = \sum_{\vec{k}} \sum_{\lambda=1,2} \hbar\omega_k \hat{a}_\lambda^\dagger(\vec{k})\hat{a}_\lambda(\vec{k}). \tag{2.3}$$

  The operators $\hat{a}_\lambda(\vec{k})$ and $\hat{a}_\lambda^\dagger(\vec{k})$ are the creation and annihilation operators for a photon in the polarization state λ, with the wave vector $\vec{k}$ and the associated angular frequency $\omega_k = c|\vec{k}|$. The assumed thermodynamic equilibrium imposes the Bose-Einstein distribution on the average photon occupancy number:

$$\langle \hat{a}_\lambda^\dagger(\vec{k})\hat{a}_{\lambda'}(\vec{k'})\rangle = \delta_{\vec{k}\vec{k'}}\delta_{\lambda\lambda'}N(\omega_k), \qquad N(\omega) = \frac{1}{\exp(\frac{\hbar\omega}{k_B T}) - 1}, \tag{2.4}$$

  where $N(\omega)$ is the average photon occupancy number at angular frequency ω and temperature T (k_B is the Boltzmann constant).

- The interaction between the bath and the open system is simplified with the dipole approximation [15],

$$\hat{H}_I = -e\hat{\vec{D}} \cdot \hat{\vec{E}}, \tag{2.5}$$

  where $\hat{\vec{D}}$ is the transition dipole operator whose complex vector elements in the energy eigenbasis we denote as $\mathbf{d}_{\epsilon\epsilon'}$,

$$\mathbf{d}_{\epsilon\epsilon'} = \left\langle \epsilon\right| \hat{\vec{D}} \left|\epsilon'\right\rangle = e \left\langle \epsilon\right| \hat{\vec{r}} \left|\epsilon'\right\rangle. \tag{2.6}$$

The operator $\hat{\vec{E}}$ is the quantized electric field operator in the Schrödinger picture,

$$\hat{\vec{E}} = i \sum_{\vec{k}} \sum_{\lambda=1,2} \sqrt{\frac{2\pi\hbar\omega_k}{V}} \left(\hat{a}_\lambda(\vec{k}) - \hat{a}_\lambda^\dagger(\vec{k}) \right) \vec{e}_\lambda, \tag{2.7}$$

where V is the finite volume of the resonator (cavity) containing the Black body radiation.

The derivation of the master equation from the von Neumann equation leads under the assumptions of weak coupling and the assumptions of the coarse-graining procedure briefly described in the previous chapter (sec. 1.2) to the following (Redfield) equation (see eq. 3.188 in [9]):

$$\frac{d}{dt}\hat{\rho}_{S_I}(t) = \sum_{\omega,\omega'} \sum_j \exp\left[i(\omega' - \omega)t\right] \gamma(\omega) \Big(\hat{A}_j(\omega)\hat{\rho}_{S_I}(t)\hat{A}_j^\dagger(\omega') - \hat{A}_j^\dagger(\omega')\hat{A}_j(\omega)\hat{\rho}_{S_I}(t) \Big) + h.c. \tag{2.8}$$

We can see that this equation is not yet in the Lindblad form (1.1) due to the factors $\exp\left[i(\omega'-\omega)t\right]$. This problem can be solved with the rotating wave approximation where we assume that the effects of the fast rotating terms ($\omega' \neq \omega$) effectively average out. To be consistent with the process of coarse-graining, we need to make sure that the timescales $\tau_{\text{RWA}} = (\omega'-\omega)^{-1}$ corresponding to the allowed transition frequencies satisfy:

$$\tau_S \gg \Delta t \gg \max(\tau_{\text{RWA}}). \tag{2.9}$$

Neglection of these terms thus requires that all of the energy levels are well spaced. We can now think of the parameter Δt also as the strength of a filter which determines the timescales over which the behaviour of the open system can be affected.

With the rotating wave approximation, the QOME (2.8) can be cast into the Lindblad form:

The quantum optical master equation

$$\frac{d}{dt}\hat{\rho}_{S_I}(t) = \sum_{\omega} \sum_j \gamma(\omega) \Big(\hat{A}_j(\omega)\hat{\rho}_{S_I}(t)\hat{A}_j^\dagger(\omega) - \hat{A}_j^\dagger(\omega)\hat{A}_j(\omega)\hat{\rho}_{S_I}(t) \Big) + h.c. \tag{2.10}$$

$$\hat{\vec{A}}(\omega) = \sum_{\hbar\omega = \epsilon' - \epsilon} |\epsilon\rangle \langle\epsilon| \vec{\hat{D}} |\epsilon'\rangle \langle\epsilon'| \tag{2.11}$$

$$\gamma(\omega) = \frac{\omega^3}{6\pi\epsilon_0\hbar c^3}(1 + N(\omega) + iS(\omega)) \tag{2.12}$$

$$S(\omega) = \frac{1}{\omega^3\pi} \mathrm{P} \int_0^\infty d\omega_k \omega_k^3 \left[\frac{1 + N(\omega_k)}{\omega - \omega_k} + \frac{N(\omega_k)}{\omega - \omega_k} \right] \tag{2.13}$$

The QOME is expressed for the density matrix $\hat{\rho}_{S_I}$ in the interaction picture and the first sum runs over all (positive and negative) angular frequencies ω_{ij} corresponding to the energy differences of the allowed transitions $E_j - E_i = \hbar\omega_{ij}$. The operators $\hat{A}_j(\omega)$ decompose the transition dipole moment operator $\hat{D}_j$ where j designates the spatial components.

Finally, the integral $S(\omega)$ in the rate coefficients $\gamma(\omega)$ accounts for the Lamb and Stark shifts and contributes to the unitary evolution [9]. The divergence of these terms $S(\omega)$ needs to be amended by renormalization. However, the sizes of these terms are generally at or below the order of the neglected terms in the weak coupling approximation and therefore we have to neglect them.

2.2 Application to V-type system in single bath

Let us calculate the equations of motion for a three-level degenerate open system coupled to a single heat bath depicted in the figure 2.1. Due to the linearity of the QOME, this calculation will actually serve as a building block for forming the equations of motion for the QHE (see fig. 3.1).

Figure 2.1: The open system consists of three states labeled $\{0, 1, 2\}$ which are represented by the black solid horizontal lines with the upper states having higher energy. The green dashed lines represent the allowed transitions between these states. These transitions are coupled to a single photon bath at temperature T which is illustrated with green arrows pointing to these transitions.

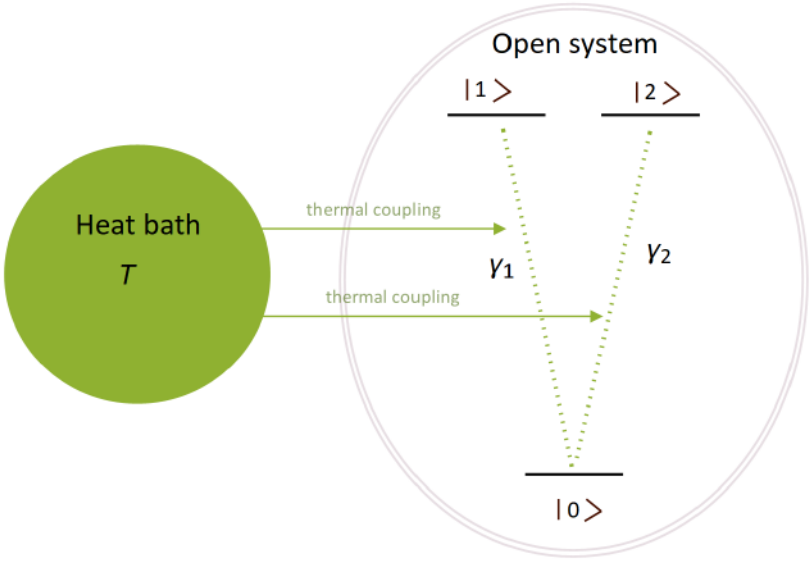

At fist, we recall the QOME presented in the preceeding section,

$$\frac{d}{dt}\hat{\rho}_{S_I}(t) = \sum_{\omega}\sum_{j}\gamma(\omega)\Big(\hat{A}_j(\omega)\hat{\rho}_{S_I}(t)\hat{A}_j^{\dagger}(\omega) - \hat{A}_j^{\dagger}(\omega)\hat{A}_j(\omega)\hat{\rho}_{S_I}(t)\Big) + h.c., \tag{2.14}$$

and take a look at the operator $\vec{\hat{A}}(\omega)$.

$$\hat{A}_j(\omega) = \sum_{\hbar\omega=\epsilon'-\epsilon} |\epsilon\rangle\langle\epsilon|\hat{D}_j|\epsilon'\rangle\langle\epsilon'| = \sum_{\hbar\omega=\epsilon'-\epsilon} |\epsilon\rangle\,\mathbf{d}_{\epsilon\epsilon'_j}\,\langle\epsilon'|\,. \tag{2.15}$$

The right-hand side of eq. (2.14) is a sum of terms where each term contributes to one spatial component. For brevity, we will omit the index j, work in one dimension and add the two remaining spatial components at the end. In the case of the element $\mathbf{d}_{\epsilon\epsilon'_j}$, we will

also omit the bold font indicating a vector and write $d_{\epsilon\epsilon'}$:

$$\hat{A}(\omega) = \sum_{\hbar\omega=\epsilon'-\epsilon} |\epsilon\rangle \langle\epsilon| \hat{D} |\epsilon'\rangle \langle\epsilon'| = \sum_{\hbar\omega=\epsilon'-\epsilon} |\epsilon\rangle d_{\epsilon\epsilon'} \langle\epsilon'| . \tag{2.16}$$

Furthermore, we notice that $\hat{A}(-\omega) = \hat{A}^\dagger(\omega)$. This formula allows us to realize that when we perform the sum over the transition frequencies $\{\omega, -\omega\}$, where $\hbar\omega = E_{12} - E_0$, we encounter only two different operators $\hat{A}$ and its hermitian conjugate $\hat{A}^\dagger$:

$$\begin{aligned}
\hat{A} &= \hat{A}(\omega) = \hat{A}^\dagger(-\omega) = |0\rangle \langle 0| \hat{D} |1\rangle \langle 1| + |0\rangle \langle 0| \hat{D} |2\rangle \langle 2| = d_{01} |0\rangle \langle 1| + d_{02} |0\rangle \langle 2| , \\
\hat{A}^\dagger &= \hat{A}(-\omega) = \hat{A}^\dagger(\omega) = |1\rangle \langle 1| \hat{D} |0\rangle \langle 0| + |2\rangle \langle 2| \hat{D} |0\rangle \langle 0| = d_{01}^* |1\rangle \langle 0| + d_{02}^* |2\rangle \langle 0| .
\end{aligned}$$

In this notation, the QOME in one spatial dimension reads:

$$\begin{aligned}
\frac{d}{dt}\hat{\rho}_{S_I} = \quad & \gamma(\omega)(2\hat{A}\hat{\rho}_{S_I}\hat{A}^\dagger - \hat{A}^\dagger\hat{A}\hat{\rho}_{S_I} - \hat{\rho}_{S_I}\hat{A}^\dagger\hat{A}) \\
& + \gamma(-\omega)(2\hat{A}^\dagger\hat{\rho}_{S_I}\hat{A} - \hat{A}\hat{A}^\dagger\hat{\rho}_{S_I} - \hat{\rho}_{S_I}\hat{A}\hat{A}^\dagger).
\end{aligned} \tag{2.17}$$

As the next step, we calculate the following terms contained in (2.17) while denoting the elements $\langle i| \hat{\rho}_{S_I} |j\rangle$ as r_{ij}:

$$\begin{aligned}
\hat{A}\hat{A}^\dagger &= (|d_{01}|^2 + |d_{02}|^2) |0\rangle \langle 0| , \\
\hat{A}^\dagger\hat{A} &= |d_{01}|^2 |1\rangle \langle 1| + |d_{02}|^2 |2\rangle \langle 2| + d_{01}^* d_{02} |1\rangle \langle 2| + d_{01} d_{02}^* |2\rangle \langle 1| , \\
\hat{A}\hat{\rho}_{S_I}\hat{A}^\dagger &= \left(|d_{01}|^2 r_{11} + |d_{02}|^2 r_{22} + d_{01}d_{02}^* r_{12} + d_{01}^* d_{02} r_{21}\right) |0\rangle \langle 0| , \\
\hat{A}^\dagger\hat{\rho}_{S_I}\hat{A} &= r_{00} \left(|d_{01}|^2 |1\rangle \langle 1| + |d_{02}|^2 |2\rangle \langle 2| + d_{01}^* d_{02} |1\rangle \langle 2| + d_{01} d_{02}^* |2\rangle \langle 1|\right) .
\end{aligned} \tag{2.18}$$

By careful observation of these terms, we notice that the elements $\{r_{01}, r_{02}\}$ and consequently their complex conjugates $\{r_{10}, r_{20}\}$ evolve independently of the other elements including the populations (diagonal elements),

$$\frac{d}{dt} r_{01} = f_1(r_{01}, r_{02}), \qquad \frac{d}{dt} r_{02} = f_2(r_{01}, r_{02}). \tag{2.19}$$

This means that we can ignore their evolution and set them to zero. Furthermore, it makes our work of transforming back into the Schrödinger picture easy because the elements $\{r_{00}, r_{11}, r_{22}, r_{12}, r_{21}\}$ which we are interested in are identical in both pictures. To see this, let us denote the elements in the Schrödinger picture as ρ_{ij}, i.e. $\rho_{ij} = \langle i| \hat{\rho}_S |j\rangle$, and denote the angular frequency proportional to the energy E_i in the formula $E = \hbar\omega$ as ω_i. The formulas for transforming between the Schrödinger and the interaction picuture are then:

$$\begin{aligned}
\rho_{ij} &= \langle i| e^{-i\hat{H}_S t/\hbar} \hat{\rho}_{I_S} e^{i\hat{H}_S t/\hbar} |j\rangle = e^{i(\omega_j - \omega_i)t} r_{ij}, \\
\frac{d}{dt}\rho_{ij} &= i(\omega_j - \omega_i)\rho_{ij} + e^{i(\omega_j - \omega_i)t} \frac{d}{dt} r_{ij}.
\end{aligned}$$

Since the upper energy levels are degenerate, $E_1 = E_2 = E_{12}$, the elements we are interested in, i.e. $\{r_{00}, r_{11}, r_{22}, r_{12}, r_{21}\}$, are indeed invariant under this transformation.

We now proceed to include the other two spatial dimensions contained in the QOME, eq. (2.14), i.e. sum over the ommited index j. In order to group this large number of terms, we will use the standard absolute value operation:

$$|\mathbf{a}|^2 = \sum_j \mathbf{a}_j \mathbf{a}_j^*,$$

and the ordinary dot product such that for two complex vectors $\mathbf{a}$ and $\mathbf{b}$ the dot product is symmetric but generally complex:

$$\mathbf{a}\cdot\mathbf{b}=\mathbf{b}\cdot\mathbf{a}=\sum_j \mathbf{a}_j\mathbf{b}_j.$$

Summation over the spatial components (x,y,z) using the equations (2.14), (2.17) and (2.18) yields:

$$\begin{aligned}\frac{d}{dt}\hat{\rho}_{S_I}=&2\gamma(\omega)\left|0\right\rangle\left\langle 0\right|\left(\left|\mathbf{d}_{01}\right|^2\rho_{11}+\left|\mathbf{d}_{02}\right|^2\rho_{22}+\mathbf{d}_{01}\cdot\mathbf{d}_{02}^*\rho_{12}+\mathbf{d}_{01}^*\cdot\mathbf{d}_{02}\rho_{21}\right)\\&+2\gamma(-\omega)\rho_{00}\left(\left|\mathbf{d}_{01}\right|^2\left|1\right\rangle\left\langle 1\right|+\left|\mathbf{d}_{02}\right|^2\left|2\right\rangle\left\langle 2\right|+\mathbf{d}_{01}^*\cdot\mathbf{d}_{02}\left|1\right\rangle\left\langle 2\right|+\mathbf{d}_{01}\cdot\mathbf{d}_{02}^*\left|2\right\rangle\left\langle 1\right|\right)\\&-\gamma(\omega)\left(\left|\mathbf{d}_{01}\right|^2\left|1\right\rangle\left\langle 1\right|+\left|\mathbf{d}_{02}\right|^2\left|2\right\rangle\left\langle 2\right|+\mathbf{d}_{01}^*\cdot\mathbf{d}_{02}\left|1\right\rangle\left\langle 2\right|+\mathbf{d}_{01}\cdot\mathbf{d}_{02}^*\left|2\right\rangle\left\langle 1\right|\right)\hat{\rho}_{S_I}\\&-\gamma(\omega)\hat{\rho}_{S_I}\left(\left|\mathbf{d}_{01}\right|^2\left|1\right\rangle\left\langle 1\right|+\left|\mathbf{d}_{02}\right|^2\left|2\right\rangle\left\langle 2\right|+\mathbf{d}_{01}^*\cdot\mathbf{d}_{02}\left|1\right\rangle\left\langle 2\right|+\mathbf{d}_{01}\cdot\mathbf{d}_{02}^*\left|2\right\rangle\left\langle 1\right|\right)\\&-\gamma(-\omega)\left(\left|\mathbf{d}_{01}\right|^2+\left|\mathbf{d}_{02}\right|^2\right)\left|0\right\rangle\left\langle 0\right|\hat{\rho}_{S_I}-\gamma(-\omega)\hat{\rho}_{S_I}\left|0\right\rangle\left\langle 0\right|\left(\left|\mathbf{d}_{01}\right|^2+\left|\mathbf{d}_{02}\right|^2\right).\end{aligned}$$

Since the uninteresting dynamics of the elements $\{\rho_{01},\rho_{02},\rho_{10},\rho_{20}\}$ can be omitted, we rearrange the QOME into a simple master equation,

$$\frac{d}{dt}\vec{\rho}=\hat{M}\vec{\rho},$$

where $\hat{M}$ is a 5×5 transition matrix acting on a vector $\vec{\rho}$ which contains the five relevant elements $\{\rho_{00},\rho_{11},\rho_{22},\rho_{12},\rho_{21}\}$. Furthermore, we simplify the transition matrix elements by making use of the property of the occupation number (defined in eq. (2.4)): $N(-\omega)=-1-N(\omega)$, and by introducing the following constants:

$$\begin{aligned}\alpha&=(3\pi\epsilon_0\hbar c^3)^{-1}, & \gamma_{12}&=\alpha\omega^3\mathbf{d}_{01}\cdot\mathbf{d}_{02}^*,\\ \gamma_1&=\alpha\omega^3\left|\mathbf{d}_{01}\right|^2, & n&=N(\omega),\\ \gamma_2&=\alpha\omega^3\left|\mathbf{d}_{02}\right|^2.\end{aligned}\tag{2.20}$$

With these constants, the master equation reads:

$$\begin{bmatrix}\dot{\rho}_{00}\\ \dot{\rho}_{11}\\ \dot{\rho}_{22}\\ \dot{\rho}_{12}\\ \dot{\rho}_{21}\end{bmatrix}=\begin{bmatrix}-(\gamma_1+\gamma_2)n & \gamma_1(1+n) & \gamma_2(1+n) & \gamma_{12}(1+n) & \gamma_{12}^*(1+n)\\ \gamma_1 n & -\gamma_1(1+n) & 0 & -\frac{\gamma_{12}}{2}(1+n) & -\frac{\gamma_{12}^*}{2}(1+n)\\ \gamma_2 n & 0 & -\gamma_2(1+n) & -\frac{\gamma_{12}}{2}(1+n) & -\frac{\gamma_{12}^*}{2}(1+n)\\ \gamma_{12}^* n & -\frac{\gamma_{12}^*}{2}(1+n) & -\frac{\gamma_{12}^*}{2}(1+n) & -\frac{\gamma_1+\gamma_2}{2}(1+n) & 0\\ \gamma_{12} n & -\frac{\gamma_{12}}{2}(1+n) & -\frac{\gamma_{12}}{2}(1+n) & 0 & -\frac{\gamma_1+\gamma_2}{2}(1+n)\end{bmatrix}\begin{bmatrix}\rho_{00}\\ \rho_{11}\\ \rho_{22}\\ \rho_{12}\\ \rho_{21}\end{bmatrix}.\tag{2.21}$$

We can introduce an even more concise notation:

$$\begin{aligned}(1+n)\gamma_1&=T_1, & n\gamma_1&=t_1,\\ (1+n)\gamma_2&=T_2, & n\gamma_2&=t_2,\\ (1+n)\gamma_{12}&=2T_{12}, & n\gamma_{12}&=2t_{12}.\end{aligned}\tag{2.22}$$

In this notation, the QOME takes the form:

$$\begin{bmatrix} \dot{\rho}_{00} \\ \dot{\rho}_{11} \\ \dot{\rho}_{22} \\ \dot{\rho}_{12} \\ \dot{\rho}_{21} \end{bmatrix} = \begin{bmatrix} -t_1 - t_2 & T_1 & T_2 & 2T_{12} & 2T_{12}^* \\ t_1 & -T_1 & 0 & -T_{12} & -T_{12}^* \\ t_2 & 0 & -T_2 & -T_{12} & -T_{12}^* \\ 2t_{12}^* & -T_{12}^* & -T_{12}^* & -(T_1+T_2)/2 & 0 \\ 2t_{12} & -T_{12} & -T_{12} & 0 & -(T_1+T_2)/2 \end{bmatrix} \begin{bmatrix} \rho_{00} \\ \rho_{11} \\ \rho_{22} \\ \rho_{12} \\ \rho_{21} \end{bmatrix}.$$

Lastly, let us note that the probability in the populations of the open system is conserved. We can verify this by summation of the first three rows of the transition matrix,

$$\frac{d}{dt}\left(\rho_{00} + \rho_{11} + \rho_{22}\right) = 0.$$

3. Quantum heat engine

We proceed by presenting the QHE model. First, we briefly describe its state cycle and outline the formation of the equations of motion from the simpler V-type system. Next, we examine the master equation and the underlying fundamental processes. This is then followed by the study of the probability currents, the energy currents and the power output of the QHE. In the last section of this chapter, we take a look at the entropy production and the efficiency.

3.1 Introduction

A quantum heat engine is a microscopic power-generating device coupled to two or more reservoirs at different temperatures. In our case, the working medium of the QHE is modeled by a five-level open system (see figure 3.1) which operates between two baths: a hot (red) and a cold (blue) bath.

Figure 3.1: A diagram of the QHE. The symbols γ_{1h}, γ_{2h}, γ_{1c}, γ_{2c}, Γ_c represent the rates of transitions coupled to the heat baths while the rate Γ represents the one-way power output of the QHE (as explained in sec. 3.9).

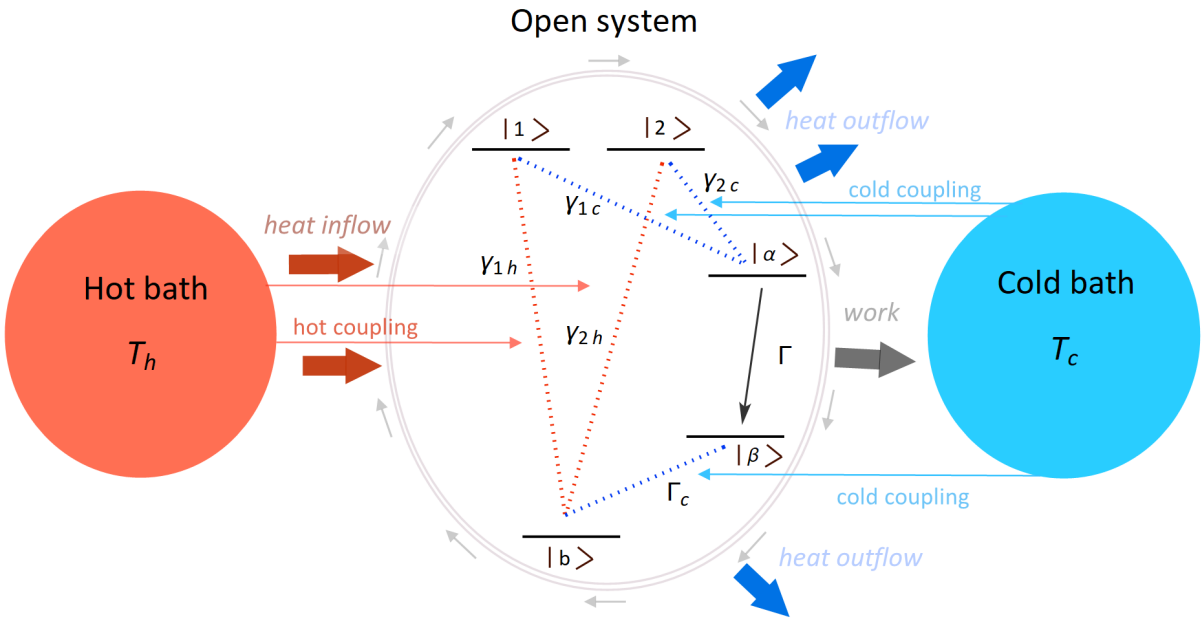

Our model corresponds to an exactly degenerate version of a quantum heat engine proposed by Dorfman et al. [8]. Their quantum heat engine is inspired by photosynthesis in plants and bacteria and models the light-dependent cycle of two tightly coupled chlorophylls at the heart of the photosynthetic reaction center. Dorfman et al. show that this model can represent artificial quantum heat engines such as a laser or a photocell [8, 14].

The open system is represented by two donor molecules and one acceptor molecule and the cycle of states of this open system (see fig. 3.1) goes as follows:

- The cycle begins with two donor molecules surrounding an acceptor molecule in the ground state $|b\rangle$.
- An absorption of a solar photon results in the excited states of the donors: $|1\rangle$ and $|2\rangle$, where the created hole and electron pair are still in the donors.
- The excited electron is then transferred from the donors to the acceptor molecule with the emission of a phonon, resulting in the charge-separated state $|\alpha\rangle$. The electron is in the acceptor molecule now and the hole remains in the donors.
- Next, the transition to $|\beta\rangle$ corresponds to the electron coming out of the acceptor molecule to some lower energy state and performing useful work. We model this process by the phenomenological rate Γ and the amount of available work in this transition depends on the ratio of the steady-state populations $\rho_{\alpha\alpha}$ and $\rho_{\beta\beta}$.
- Finally, the positive charge is neutralized by an electron source with the emission of a phonon. The open system returns to the ground state $|b\rangle$.

It turns out that their proposed model suffers from a violation of positivity and divergent behavior [14]. We adopt the same scheme of the QHE with the difference that the upper energy levels are perfectly degenerate and we use a QOME in the Lindblad form. This model then ensures the properties of the density matrix.

3.2 Equations of motion

Let us proceed by calculating the equations of motion for the QHE. First, we take a look at the allowed transitions in fig. 3.1 which determine the form of the transition dipole moment operator $\vec{\hat{D}}$:

$$\vec{\hat{D}} = \begin{bmatrix} 0 & \mathbf{d}_{b1} & \mathbf{d}_{b2} & 0 & \mathbf{d}_{b\beta} \\ \mathbf{d}_{b1}^* & 0 & 0 & \mathbf{d}_{\alpha 1} & 0 \\ \mathbf{d}_{b2}^* & 0 & 0 & \mathbf{d}_{\alpha 2} & 0 \\ 0 & \mathbf{d}_{\alpha 1}^* & \mathbf{d}_{\alpha 2}^* & 0 & 0 \\ \mathbf{d}_{b\beta}^* & 0 & 0 & 0 & 0 \end{bmatrix}. \tag{3.1}$$

Note that we order the state basis in the matrix representation clockwise in the QHE cycle starting with the ground state b, i.e. $\{b, 1, 2, \alpha, \beta\}$. The transition between the states $\{\alpha, \beta\}$ is neglected for now and will be added at the very end.

The allowed transitions determine the set of the transition frequencies which we sum over in the QOME. These include the angular frequencies $\{\omega_{b12}, \omega_{\alpha 12}, \omega_{b\beta}\}$ where ω_{AB} denotes the frequency corresponding to the energy difference $E_B - E_A = \hbar\omega_{AB}$. We can think of the sum over different transition frequencies as a sum over different subsystems. In our case, we have two V-type systems: $\hat{K}(\omega_{b12}, T_h)$ and $\hat{K}(\omega_{\alpha 12}, T_c)$ operating between the states $\{b, 1, 2\}$ and $\{\alpha, 1, 2\}$ respectively, and a two-level system $\hat{K}(\omega_{b\beta}, T_c)$ operating between $\{b, \beta\}$. These systems are coupled to their respective baths, i.e. the hot (T_h) or the cold (T_c) bath, and add up to form the QHE model:

$$\begin{aligned} \frac{d}{dt}\hat{\rho}_S =& \hat{K}(\omega_{b12}, T_h) + \hat{K}(\omega_{\alpha 12}, T_c) + \hat{K}(\omega_{b\beta}, T_c), \\ \hat{K}(\omega, T) =& \gamma(\omega, T)(2\hat{A}\hat{\rho}_{S_I}\hat{A}^\dagger - \hat{A}^\dagger\hat{A}\hat{\rho}_{S_I} - \hat{\rho}_{S_I}\hat{A}^\dagger\hat{A}) \\ &+ \gamma(-\omega, T)(2\hat{A}^\dagger\hat{\rho}_{S_I}\hat{A} - \hat{A}\hat{A}^\dagger\hat{\rho}_{S_I} - \hat{\rho}_{S_I}\hat{A}\hat{A}^\dagger). \end{aligned}$$

Note that the expression for $\hat{K}(\omega, T)$ is written in one dimension, as in eq. (2.17). In order to arrive at the equations for the two-level system, it is convenient to consider the equations for a three-level V-type system and set one of the transition dipole moments to zero.

Besides the populations, the relevant reduced density matrix elements of the subsystems only include the coherences ρ_{12} and ρ_{21} (which arise in the calculation for the V-type system):

$$\hat{\rho}_S = \begin{bmatrix} \rho_{bb} & \rho_{b1} & \rho_{b2} & \rho_{b\alpha} & \rho_{b\beta} \\ \rho_{1b} & \rho_{11} & \rho_{12} & \rho_{1\alpha} & \rho_{1\beta} \\ \rho_{2b} & \rho_{21} & \rho_{22} & \rho_{2\alpha} & \rho_{2\beta} \\ \rho_{\alpha b} & \rho_{\alpha 1} & \rho_{\alpha 2} & \rho_{\alpha\alpha} & \rho_{\alpha\beta} \\ \rho_{\beta b} & \rho_{\beta 1} & \rho_{\beta 2} & \rho_{\beta\alpha} & \rho_{\beta\beta} \end{bmatrix}. \tag{3.2}$$

We will arrange the relevant elements (black) into a master equation and order the elements in the state vector $\vec{\rho}$ such that the coherences are at the end:

$$\frac{d}{dt}\vec{\rho} = \hat{M}\vec{\rho}, \qquad \vec{\rho} = (\rho_{bb}, \rho_{11}, \rho_{22}, \rho_{\alpha\alpha}, \rho_{\beta\beta}, \rho_{12}, \rho_{21})^T. \tag{3.3}$$

For a concise description, let us introduce constants analogous to the ones for the V-type system (2.20):

$$\begin{aligned} \gamma_{1h} &= \alpha\omega_{b12}^3 \left|\mathbf{d}_{b1}\right|^2, & \gamma_{12h} &= \alpha\omega_{b12}^3 \mathbf{d}_{b1}\cdot\mathbf{d}_{b2}^*, & n_h &= N(\omega_{b12}, T_h), \\ \gamma_{2h} &= \alpha\omega_{b12}^3 \left|\mathbf{d}_{b2}\right|^2, & \gamma_{12c} &= \alpha\omega_{\alpha 12}^3 \mathbf{d}_{\alpha 1}\cdot\mathbf{d}_{\alpha 2}^*, & n_c &= N(\omega_{\alpha 12}, T_c), \\ \gamma_{1c} &= \alpha\omega_{\alpha 12}^3 \left|\mathbf{d}_{\alpha 1}\right|^2, & \Gamma_c &= \alpha\omega_{b\beta}^3 \left|\mathbf{d}_{b\beta}\right|^2, & N_c &= N(\omega_{b\beta}, T_c), \\ \gamma_{2c} &= \alpha\omega_{\alpha 12}^3 \left|\mathbf{d}_{\alpha 2}\right|^2, & \alpha &= (3\pi\epsilon_0\hbar c^3)^{-1}. \end{aligned} \tag{3.4}$$

We further group these constants together:

$$\begin{aligned} (1+n_h)\gamma_{1h} &= H_1, & (1+n_c)\gamma_{1c} &= C_1, & n_c\gamma_{1c} &= c_1, & n_h\gamma_{1h} &= h_1, \\ (1+n_h)\gamma_{2h} &= H_2, & (1+n_c)\gamma_{2c} &= C_2, & n_c\gamma_{2c} &= c_2, & n_h\gamma_{2h} &= h_2, \\ (1+n_h)\gamma_{12h} &= 2H_{12}, & (1+n_c)\gamma_{12c} &= 2C_{12}, & n_c\gamma_{12c} &= 2c_{12}, & n_h\gamma_{12h} &= 2h_{12}, \\ & & (1+N_c)\Gamma_c &= C_0, & N_c\Gamma_c &= c_0. \end{aligned} \tag{3.5}$$

In addition to the transitions governed by the QOME, we describe the one-way transition between the states $\{\alpha, \beta\}$ by a non-negative transition rate Γ. During this transition, part of the energy transfer corresponds to useful work and therefore the rate Γ controls the power output of the QHE, see fig. 3.1 and sec. 3.9. To test the stability of the result, we also include a phenomenological decoherence rate modeling the decay of the coherence elements ρ_{12} and ρ_{21}. These two phenomenological effects correspond to the following dynamics:

$$\begin{bmatrix} \dot{\rho}_{\alpha\alpha} \\ \dot{\rho}_{\beta\beta} \end{bmatrix} = \begin{bmatrix} -\Gamma & 0 \\ 0 & +\Gamma \end{bmatrix} \begin{bmatrix} \rho_{\alpha\alpha} \\ \rho_{\beta\beta} \end{bmatrix}, \qquad \begin{bmatrix} \dot{\rho}_{12} \\ \dot{\rho}_{21} \end{bmatrix} = \begin{bmatrix} -\Lambda/2 & 0 \\ 0 & -\Lambda/2 \end{bmatrix} \begin{bmatrix} \rho_{12} \\ \rho_{21} \end{bmatrix}. \tag{3.6}$$

The transition matrix of the the resulting master equation reads:

$$\hat{M} = \begin{bmatrix} -c_0-h_1-h_2 & H_1 & H_2 & 0 & C_0 & 2H_{12} & 2H_{12}^* \\ h_1 & -C_1-H_1 & 0 & c_1 & 0 & -C_{12}-H_{12} & -C_{12}^*-H_{12}^* \\ h_2 & 0 & -C_2-H_2 & c_2 & 0 & -C_{12}-H_{12} & -C_{12}^*-H_{12}^* \\ 0 & C_1 & C_2 & -c_1-c_2-\Gamma & 0 & 2C_{12} & 2C_{12}^* \\ c_0 & 0 & 0 & \Gamma & -C_0 & 0 & 0 \\ 2h_{12}^* & -C_{12}^*-H_{12}^* & -C_{12}^*-H_{12}^* & 2c_{12}^* & 0 & \begin{matrix}-(C_1+C_2+\\+H_1+H_2+\Lambda)/2\end{matrix} & 0 \\ 2h_{12} & -C_{12}-H_{12} & -C_{12}-H_{12} & 2c_{12} & 0 & 0 & \begin{matrix}-(C_1+C_2+\\+H_1+H_2+\Lambda)/2\end{matrix} \end{bmatrix}. \tag{3.7}$$

Lastly, we see that the probality in the populations $\sum_i \rho_{ii}$ is conserved:

$$\sum_i \frac{d}{dt}\rho_{ii}(t) = 0. \tag{3.8}$$

3.3 Solutions to the master equation

The obtained master equation is a system of first-order linear homogeneous differential equations:

$$\frac{d}{dt}\vec{\rho} = \hat{M}\vec{\rho}. \tag{3.9}$$

The evolution of a specific initial state $\vec{\rho}(t_0)$ from time t_0 to t is governed by the propagator $\hat{U}_M(t, t_0)$:

$$\vec{\rho}(t) = \hat{U}_M(t, t_0)\vec{\rho}(t_0) = \exp\left[\vec{M}(t - t_0)\right]\vec{\rho}(t_0). \tag{3.10}$$

We can obtain the steady-state solutions $\vec{\rho}_{st}$ from the null space of the transition matrix $\ker(\hat{M})$:

$$\frac{d}{dt}\vec{\rho}_{st} = \hat{M}\vec{\rho}_{st} = 0. \tag{3.11}$$

The steady-state vectors $\vec{\rho}_{st}$ do not evolve in time and therefore depend only on the parameters determining the matrix $\hat{M}$. These can be expressed using the rates Γ and Λ, the temperatures T_h and T_c, the energies E_b, E_α, E_{12} and E_β, and the transition dipole moments $\mathbf{d}_{b1}$, $\mathbf{d}_{b2}$, $\mathbf{d}_{\alpha 1}$, $\mathbf{d}_{\alpha 2}$ and $\mathbf{d}_{b\beta}$. We shall call the sets of parameters determining the steady-state vector

$$\vec{\rho}_{st} = \vec{\rho}_{st}(\Gamma, T_h, T_c, E_b, E_{12}, E_\alpha, E_\beta, \mathbf{d}_{b1}, \mathbf{d}_{b2}, \mathbf{d}_{\alpha 1}, \mathbf{d}_{\alpha 2}, \mathbf{d}_{b\beta}, \Lambda),$$

the *model parameters*. Usually, one expects the nullspace of $\hat{M}$ to be one-dimensional. However, as we shall see later, constraints on the coefficiets of the transition matrix $\hat{M}$ can result in a more than one-dimensional null space. The significance of these additional steady-state solutions will be discussed separately (see secs. 4.1, 4.3, 4.6).

3.4 Fundamental processes

To interpret the equations of motion, we recall the Einstein coefficients [16] A and B corresponding to the processes of spontaneous emission and stimulated emission and absorbtion. The following equations describe these processes in a system with $N_0 + N_1$ atoms interacting with electromagnetic radiation in thermodynamic equilibrium where N_0 is the number of atoms in the ground state and N_1 is the number of atoms in the excited state:

$$\left[\frac{dN_0}{dt}\right]_{abs} = -u(\omega,T)BN_1 = -\left[\frac{dN_1}{dt}\right]_{abs}, \tag{3.12}$$

$$\left[\frac{dN_1}{dt}\right]_{stim} = -u(\omega,T)BN_1 = -\left[\frac{dN_0}{dt}\right]_{stim}, \tag{3.13}$$

$$\left[\frac{dN_1}{dt}\right]_{spont} = -AN_1 = -\left[\frac{dN_0}{dt}\right]_{spont}. \tag{3.14}$$

The function $u(\omega,T)$ is the spectral energy density at angular frequency ω and temperature T given by Planck's law of black body radiation,

$$u(\omega,T) = \frac{2\hbar\omega^3}{\pi c^3}\frac{1}{\exp\left(\frac{\hbar\omega}{k_bT}\right)-1} = \frac{A}{B}N(\omega). \tag{3.15}$$

It is an interesting fact that the spontaneous emission is temperature independent and causes an exponential decay of the excited state, whereas the stimulated processes depend on the spectral energy density. Furthermore, the spontaneous emission can be regarded as the stimulated emission process caused by a virtual photon coming from vacuum fluctuations. The phase, the polarization and the direction of propagation of the emitted photon are then random, unlike in the process of stimulated emission where the emitted photon is created in the same state as the real stimulating photon [16].

Summation of the processes $(3.12-3.14)$ and a rearrangment yields:

$$\begin{aligned}\left(\frac{dN_1}{dt}\right) = -\left(\frac{dN_0}{dt}\right) &= \left(\frac{dN_1}{dt}\right)_{abs} + \left(\frac{dN_1}{dt}\right)_{stim} + \left(\frac{dN_1}{dt}\right)_{spont} \\ &= A[\frac{B}{A}u(\nu)N_0 - (1+\frac{B}{A}u(\nu))N_1] \\ &= A[N(\omega)N_0 - (1+N(\omega))N_1],\end{aligned}$$

which can be put into a matrix form:

$$\frac{d}{dt}\begin{bmatrix}N_0\\N_1\end{bmatrix} = A\begin{bmatrix}-N(\omega) & (1+N(\omega))\\ N(\omega) & -(1+N(\omega))\end{bmatrix}\begin{bmatrix}N_0\\N_1\end{bmatrix}. \tag{3.16}$$

This 2×2 matrix allows us to see the footprints of the processes $(3.12-3.14)$ in the transition matrix:

$$\hat{M} =$$

	ρ_{bb}	ρ_{11}	ρ_{22}	$\rho_{\alpha\alpha}$	$\rho_{\beta\beta}$	ρ_{12}	ρ_{21}
$\dot{\rho}_{bb}$	$-c_0-h_1-h_2$	H_1	H_2	0	C_0	$2H_{12}$	$2H^*_{12}$
$\dot{\rho}_{11}$	h_1	$-C_1-H_1$	0	c_1	0	$-C_{12}-H_{12}$	$-C^*_{12}-H^*_{12}$
$\dot{\rho}_{22}$	h_2	0	$-C_2-H_2$	c_2	0	$-C_{12}-H_{12}$	$-C^*_{12}-H^*_{12}$
$\dot{\rho}_{\alpha\alpha}$	0	C_1	C_2	$-c_1-c_2-\Gamma$	0	$2C_{12}$	$2C^*_{12}$
$\dot{\rho}_{\beta\beta}$	c_0	0	0	Γ	$-C_0$	0	0
$\dot{\rho}_{12}$	$2h^*_{12}$	$-C^*_{12}-H^*_{12}$	$-C^*_{12}-H^*_{12}$	$2c^*_{12}$	0	$-(C_1+C_2+$ $+H_1+H_2+\Lambda)/2$	0
$\dot{\rho}_{21}$	$2h_{12}$	$-C_{12}-H_{12}$	$-C_{12}-H_{12}$	$2c_{12}$	0	0	$-(C_1+C_2+$ $+H_1+H_2+\Lambda)/2$

(3.17)

Specifically, we can compare the form of the equation (3.16) with the coefficients in the upper left 5×5 part of the transition matrix in eq. (3.17).[1] From the definition of the coefficients, see eqs. (3.4) and (3.5), we check that the processes are indeed contained in the transition matrix. For example, the coefficients in red correspond to the transition between the states $\{b, 1\}$ where the rate H_1 is the rate of the emission process (both stimulated and spontaneous emission) and the rate h_1 is the rate of absorption.

The presence of these processes can be further supported by checking the standard result that in the dipole approximation the rate of spontaneous emission is proportional to the square of the transition dipole moment, see eqs. (3.4) and (3.5).

Notice that the rates of emission $\{C_1, C_2, H_1, H_2\}$ from the upper states contribute to the decay of the coherences.

3.5 Alignment of transition dipole moments

Besides the dynamics in the upper left 5×5 part of the transition matrix in eq. (3.17), we have terms describing the coherent part of the fundamental processes arising from the degeneracy of the upper energy levels. The rate constants $\{c_{12}, C_{12}\}$ and $\{h_{12}, H_{12}\}$ are proportional to the dot products of the transition dipole moments $\mathbf{d}_{\alpha 1} \cdot \mathbf{d}^*_{\alpha 2}$ and $\mathbf{d}_{b1} \cdot \mathbf{d}^*_{b2}$ respectively, see eqs. (3.4) and (3.5). The values of these dot products clearly affect the behaviour of the coherences and if we set them to zero, the open system is always in a non-coherent state ($\rho_{12} = \rho_{21} = 0$). We can also push the open system towards a non-coherent state by increasing the decoherence rate Λ. Therefore, we call either of these cases where $c_{12} = C_{12} = h_{12} = H_{12} = 0$ or $\Lambda \to \infty$ the *no coherence* case.

3.6 Probability currents

The conservation of probability tells us that the changes in the populations are caused by the flow of probability, i.e. probability currents. Let us denote a probability current

[1] The added top row and left column in eq. (3.17) serve for better orientation in the transition matrix.

from the population ρ_{ii} to ρ_{kk} as j_{ik}. The conservation of probability then reads:

$$\frac{d}{dt}\rho_{ii}(t) = -\sum_{k\neq i} j_{ik}(t) = \sum_{k\neq i} j_{ki}(t), \tag{3.18}$$

where we have used the property $j_{ik}(t) = -j_{ki}(t)$ of currents. We are defining probability currents between populations only and thus we can restrict ourselves to the first five rows of the transition matrix:[2]

$$\begin{array}{c} \\ \dot\rho_{bb} \\ \dot\rho_{11} \\ \dot\rho_{22} \\ \dot\rho_{\alpha\alpha} \\ \dot\rho_{\beta\beta} \end{array}
\begin{array}{c}
\begin{array}{ccccccc} \rho_{bb} & \rho_{11} & \rho_{22} & \rho_{\alpha\alpha} & \rho_{\beta\beta} & \rho_{12} & \rho_{21} \end{array} \\
\left[\begin{array}{ccccccc}
-c_0-h_1-h_2 & H_1 & H_2 & 0 & C_0 & 2H_{12} & 2H_{12}^* \\
h_1 & -C_1-H_1 & 0 & c_1 & 0 & -C_{12}-H_{12} & -C_{12}^*-H_{12}^* \\
h_2 & 0 & -C_2-H_2 & c_2 & 0 & -C_{12}-H_{12} & -C_{12}^*-H_{12}^* \\
0 & C_1 & C_2 & -c_1-c_2-\Gamma & 0 & 2C_{12} & 2C_{12}^* \\
c_0 & 0 & 0 & \Gamma & -C_0 & 0 & 0
\end{array}\right]
\end{array}.$$

In the no coherence case, we can identify the probability currents, i.e. trace the changes in the populations, by following the fundamental processes. The probability current j_{ik} then has the form:

$$j_{ik}(|\mathbf{d}_{ik}|^2) = \gamma_1(|\mathbf{d}_{ik}|^2)\rho_{ii} - \gamma_2(|\mathbf{d}_{ik}|^2)\rho_{kk},$$

where the rates γ_1 and γ_2 are proportional to the square of the transition dipole moment $|\mathbf{d}_{ik}|^2$. As an example, the probability current between the states $\{b, \beta\}$ reads:

$$\begin{aligned} j_{b\beta} &= c_0\rho_{bb} - C_0\rho_{\beta\beta} \\ &= \alpha\omega_{b\beta}^3 \left|\mathbf{d}_{b\beta}\right|^2 (N_c\rho_{bb} - (1+N_c)\rho_{\beta\beta}). \end{aligned}$$

The special case is the transition between the states $\{\alpha, \beta\}$ which is not modeled with simple absorption and emission processes. It is modeled so that the rate of excitation from β to α is zero and the rate of deexcitation is governed by the rate Γ,

$$j_{\alpha\beta} = \Gamma\rho_{\alpha\alpha}.$$

In the general case, the populations are also affected by terms proportional to the dot products of the transition dipole moments, $\mathbf{d}_{\alpha 1}\cdot\mathbf{d}_{\alpha 2}^*$ and $\mathbf{d}_{b1}\cdot\mathbf{d}_{b2}^*$, and the coherences ρ_{12} and ρ_{21}. These terms arise because of coherent excitation to the upper degenerate levels $\{1, 2\}$, i.e. when the open system is excited into a superposition of these states. The conservation of probability tells us that these terms must modify the sums of the probability currents $j_{b1} + j_{\alpha 1}$ and $j_{b2} + j_{\alpha 2}$ connected to these levels:

$$\begin{aligned} \dot\rho_{11} &= j_{b1} + j_{\alpha 1} = h_1\rho_{bb} + c_1\rho_{\alpha\alpha} - (C_1 + H_1)\rho_{11} - (C_{12} + H_{12})\rho_{12} - (C_{12}^* + H_{12}^*)\rho_{21}, \\ \dot\rho_{22} &= j_{b2} + j_{\alpha 2} = h_2\rho_{bb} + c_2\rho_{\alpha\alpha} - (C_2 + H_2)\rho_{11} - (C_{12} + H_{12})\rho_{12} - (C_{12}^* + H_{12}^*)\rho_{21}. \end{aligned}$$

We can split these new terms by distinguishing between the hot and cold V-type systems, such that the currents j_{b1} and j_{b2} now also have terms proportional to $\mathbf{d}_{b1}\cdot\mathbf{d}_{b2}^*$, and $j_{\alpha 1}$ and $j_{\alpha 2}$ terms proportional to $\mathbf{d}_{\alpha 1}\cdot\mathbf{d}_{\alpha 2}^*$. Finally, we write down the probability currents

[2] The added top row and left column serve for better orientation in the transition matrix.

in the general case:

$$\begin{aligned}
j_{b1}(|\mathbf{d}_{b1}|^2, \mathbf{d}_{b1}\cdot\mathbf{d}_{b2}^*) &= h_1\rho_{bb} - H_1\rho_{11} - H_{12}\rho_{12} - H_{12}^*\rho_{21},\\
j_{b2}(|\mathbf{d}_{b2}|^2, \mathbf{d}_{b1}\cdot\mathbf{d}_{b2}^*) &= h_2\rho_{bb} - H_2\rho_{22} - H_{12}\rho_{12} - H_{12}^*\rho_{21},\\
j_{\alpha1}(|\mathbf{d}_{\alpha1}|^2, \mathbf{d}_{\alpha1}\cdot\mathbf{d}_{\alpha2}^*) &= c_1\rho_{\alpha\alpha} - C_1\rho_{11} - C_{12}\rho_{12} - C_{12}^*\rho_{21},\\
j_{\alpha2}(|\mathbf{d}_{\alpha2}|^2, \mathbf{d}_{\alpha1}\cdot\mathbf{d}_{\alpha2}^*) &= c_2\rho_{\alpha\alpha} - C_2\rho_{22} - C_{12}\rho_{12} - C_{12}^*\rho_{21},\\
j_{b\beta}(|\mathbf{d}_{b\beta}|^2) &= c_0\rho_{bb} - C_0\rho_{\beta\beta},\\
j_{\alpha\beta}(\Gamma) &= \Gamma\rho_{\alpha\alpha}.
\end{aligned} \tag{3.19}$$

If we merge the states $\{1,2\}$, the transitions between the energy levels form a single loop, see fig. 3.1. For this single loop, the conservation of probability in the steady state implies that there exists a single steady-state current j which we define in the clockwise direction (in the QHE diagram),

$$j \overset{\text{s.s.}}{=} j_{\alpha\beta} \overset{\text{s.s.}}{=} j_{\beta b} \overset{\text{s.s.}}{=} j_{b1} + j_{b2} \overset{\text{s.s.}}{=} j_{1\alpha} + j_{2\alpha}, \tag{3.20}$$

Lastly, it is convenient to notice that the shortest expression for the steady-state current j is the eq. (3.19).

3.7 Energy currents

We define an energy current u_{AB} as the probability current j_{AB} multiplied by the energy change $E_B - E_A$ during the transition,

$$u_{AB} = j_{AB}(E_B - E_A). \tag{3.21}$$

For positive steady-state current $j > 0$ and for baths with different temperatures such that $T_h > T_c$, we group together the energy currents to form the average heat flowing in (q_{in}) and out (q_{out}) of the open system:

$$\begin{aligned}
q_{in} = u_{b12} &= j_{b12}(E_{12} - E_b)\\
&\overset{\text{s.s.}}{=} j(E_{12} - E_b), &(3.22)\\
q_{out} = u_{12\alpha} + u_{\beta b} &= -j_{\alpha12}(E_{12} - E_\alpha) - j_{b\beta}(E_\beta - E_b)\\
&\overset{\text{s.s.}}{=} j(E_{12} - E_\alpha + E_\beta - E_b). &(3.23)
\end{aligned}$$

We have ommited the one-way transition between the levels $\{\alpha, \beta\}$ controlled by the rate Γ which we assume consists of both power output (p_{out}) and heat outflow ($\widetilde{q}_{out}$):

$$\begin{aligned}
p_{out} + \widetilde{q}_{out} = u_{\alpha\beta} &= j_{\alpha\beta}(E_\alpha - E_\beta)\\
&\overset{\text{s.s.}}{=} j(E_\alpha - E_\beta).
\end{aligned} \tag{3.24}$$

The conservation of energy in the open system then reads:

$$u = q_{in} - q_{out} - \widetilde{q}_{out} - p_{out} = 0. \tag{3.25}$$

It follows immediately that the conservation of energy in the open system must hold in the steady state:

$$\dot{u} \overset{\text{s.s.}}{=} 0.$$

3.8 Available work at constant temperature

The available energy (useful work) at constant temperature corresponds to the change in the Helmholtz free energy, $F = U - TS$,

$$đW = dF|_T = dU|_T + TdS. \tag{3.26}$$

If we view the transition $\{\alpha, \beta\}$ as a thermodynamic process at constant temperature (T_c), the available energy $\Delta F_{\alpha\to\beta}$ along this transition then corresponds to the energy difference corrected by the change of entropy [17],

$$\begin{aligned}\Delta F_{\alpha\to\beta} &= E_\alpha - E_\beta - T_c(\Delta S_{\alpha\to\beta}) \\ &= E_\alpha - E_\beta - T_c(-k_B \log \rho_{\alpha\alpha} + k_B \log \rho_{\beta\beta}) \\ &= E_\alpha - E_\beta + k_B T_c \log \tfrac{\rho_{\alpha\alpha}}{\rho_{\beta\beta}}.\end{aligned} \tag{3.27}$$

When Γ is zero, the steady-state current through the open system vanishes (the QHE loop is broken). We shall refer to this state as the *open circuit* and refer to the associated voltage and free energy as the open circuit voltage V_{oc} and the open circuit free energy ΔF_{oc},

$$\begin{aligned}eV_{oc} = \Delta F_{oc} &= \Delta F_{\alpha\to\beta}(\Gamma = 0, T_h, T_c, E_b, ..., \mathbf{d}_{b1}, ..., \tau) \\ &= E_\alpha - E_\beta + k_B T_c \log \tfrac{\rho_{\alpha\alpha}}{\rho_{\beta\beta}}\Big|_{\Gamma=0}.\end{aligned} \tag{3.28}$$

To extract the available energy we allow the open system to transition from α to β by increasing the rate Γ from zero. The power output p_{out} of the QHE is then calculated as the probability current multiplied by the available energy and we note that this yields the standard formula for electrical power output:

$$p_{out}(\Gamma) = j_{\alpha\beta}\Delta F_{\alpha\to\beta} \overset{\text{s.s.}}{=} jeV. \tag{3.29}$$

3.9 Work rate of the engine

By varying the phenomenological rate Γ with all other steady-state parameters fixed, we explore different loads across the transition $\{\alpha, \beta\}$ and discover the current-voltage characteristic of the QHE. Let us, therefore, consider the possible values of the rate Γ. We only assume non-negative values but we also expect that there exists an upper-bound Γ_{max} due to our requirement that the available energy is not negative:

$$\Delta F_{\alpha\to\beta}(\Gamma) \geq 0. \tag{3.30}$$

This is because the rate Γ governs the current and is able to lower the voltage (available energy) to negative values which corresponds to an input of energy into the open system. As another example, consider the steady state with equal temperatures, $T_c = T_h$. A positive value of Γ would move the open system out of thermodynamic equilibrium and this would again require an input of energy.

3.10 Entropy and efficiency

The total entropy production s_{tot} consists of the entropy changes in the open system s_{sys} and the changes in the baths s_{baths},

$$s_{tot} = s_{sys} + s_{baths}. \tag{3.31}$$

We can track the entropy changes in the baths by following the heat exchanges:

$$s_{baths} = \frac{q_{out} + \widetilde{q}_{out}}{T_c} - \frac{q_{in}}{T_h}. \tag{3.32}$$

On the other hand, there are many ways to quantify the entropy changes in the open system such as von Neumanns' entropy. Nevertheless, if we restrict our interest to the steady state, the reduced density matrix $\hat{\rho}_S$ stays constant and consequently the entropy of the open system too. The entropy production in the steady state thus reads:

$$s_{tot} \overset{\text{s.s.}}{=} j \left(\frac{E_{12} - E_b - \Delta F_{\alpha\to\beta}}{T_c} - \frac{E_{12} - E_b}{T_h} \right). \tag{3.33}$$

Since we assume only non-negative currents, the second product in the parentheses must be also non-negative (due to the second law of thermodynamics). This requirement yields the bound on the voltage which corresponds to the Carnot limit η_c on efficiency of the QHE η:

$$\begin{aligned} \Delta F_{\alpha\to\beta} &\leq (E_{12} - E_b)(1 - T_c/T_h), \\ \eta = \frac{p_{out}}{q_{in}} = \frac{\Delta F_{\alpha\to\beta}}{E_{12} - E_b} &\leq 1 - T_c/T_h = \eta_c. \end{aligned} \tag{3.34}$$

Because any current necessarily lowers the voltage, it follows that the current vanishes at the maximum voltage V_{oc} corresponding to zero entropy production. Therefore we have:

$$eV_{oc} = \Delta F_{oc} = (E_{12} - E_b)(1 - T_c/T_h). \tag{3.35}$$

This is illustrated with example model parameters in fig. 3.2.

Figure 3.2: a) The current-voltage characteristic (red) obtained by variation of Γ for model parameters A (see Appendix) which include $T_c = 300\,\mathrm{K}$, $T_h = 6000\,\mathrm{K}$, in the no coherence case. The current rises significantly for voltages close to the open circuit but soon reaches a point where it slowly converges to its maximum value at zero voltage.
b) The efficiency (violet) is proportional to the voltage, see eq. (3.34), and approaches the Carnot limit η_c (black) where the current vanishes.

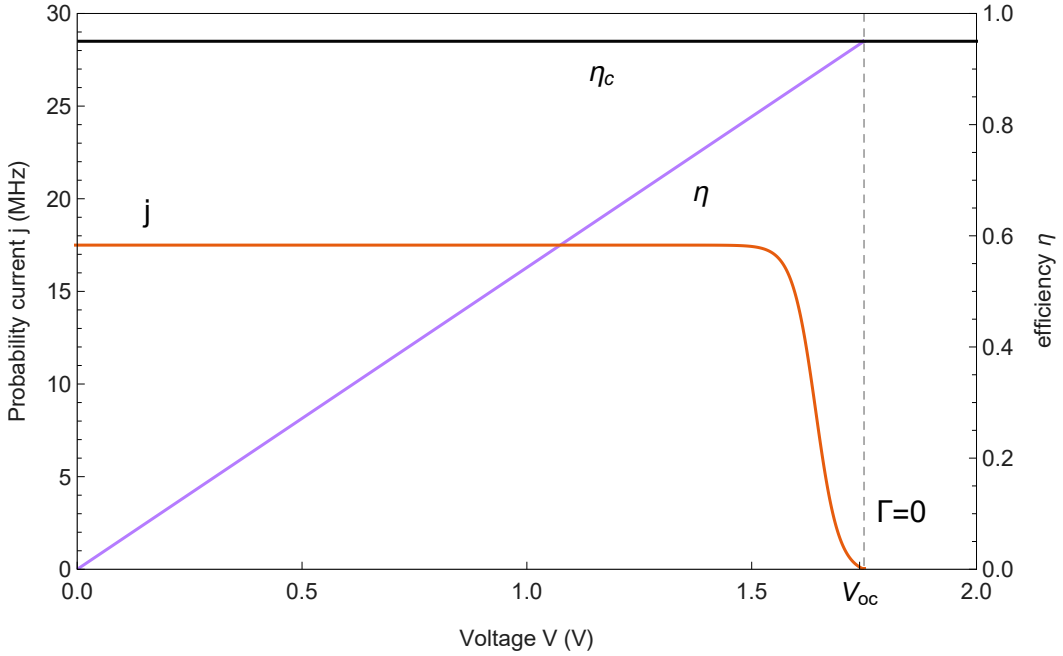

Let us note that when we assume a small steady-state current, i.e. an efficient QHE, we find that the power output becomes approximately proportional to the current (see figure 3.3),

$$p_{out} = j\Delta F_{\alpha\to\beta} \approx jeV_{oc} \approx j(E_{12} - E_b)(1 - T_c/T_h).$$

For devices operating near the open circuit, one therefore tries to maximize the current.

Figure 3.3: a) The current-voltage characteristic (red) obtained by variation of Γ for model parameters A (see Appendix), in the no coherence case.
b) The power output p_{out} (blue) of the QHE.

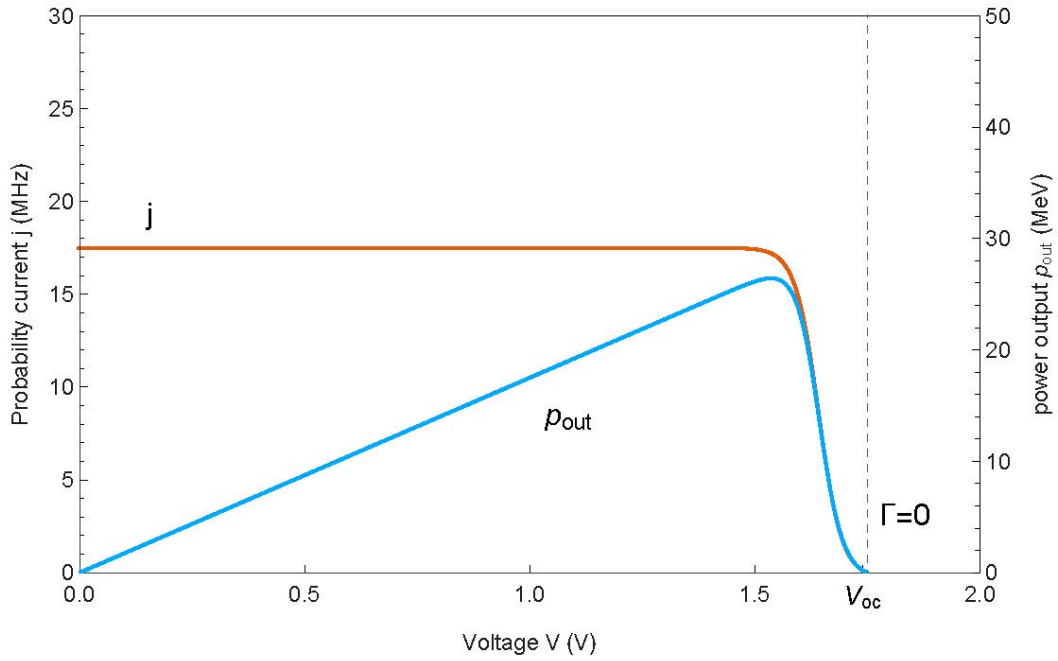

The current-voltage characteristics shown in figures 3.2 and 3.3 strongly resemble the current-voltage characteristics of solar cells [18] and one can, therefore, associate the variation of the rate Γ to the variation of electrical resistance in solar cells.

4. Coherence

We now turn our attention to the effects of coherence in the steady state. To simplify the analysis, we will follow the approximations performed by Dorfman et al. (in [8]) which will substantially reduce the number of parameters. Before that, however, we take a look at the phenomenon called the *dark state* and introduce a parametrization of the rates affecting coherence.

4.1 Dark state of V-type system

Let us restrict ourselves to the simple V-type 3-level open system, presented in section 2.2. The steady state can be determined by just 4 parameters $\{n, \gamma_1, \gamma_2, \gamma_{12}\}$,

$$n = \frac{1}{\exp(\frac{\hbar\omega}{k_B T}) - 1}, \qquad \gamma_1 = \alpha\omega^3 \left|\mathbf{d}_{01}\right|^2, \qquad \gamma_2 = \alpha\omega^3 \left|\mathbf{d}_{02}\right|^2, \qquad \gamma_{12} = \alpha\omega^3 \mathbf{d}_{01} \cdot \mathbf{d}_{02}^*,$$

where the rate γ_{12} is generally complex and its modulus is bounded by the Cauchy-Schwartz inequality,

$$|\gamma_{12}| = \alpha\omega^3 \left|\mathbf{d}_{01} \cdot \mathbf{d}_{02}^*\right| \leq \alpha\omega^3 \left|\mathbf{d}_{01}\right| \left|\mathbf{d}_{02}\right|.$$

We introduce a parameter $\delta \in \langle -1, 1\rangle$ to control the relative strengths of the rates γ_1 and γ_2 and then we restrict γ_{12} to its maximum modulus with and an arbitrary phase φ:

$$\gamma_1 = \gamma(1+\delta), \qquad \gamma_2 = \gamma(1-\delta), \qquad \gamma_{12} = \sqrt{\gamma_1\gamma_2}e^{i\varphi} = \gamma\sqrt{(1+\delta)(1-\delta)}e^{i\varphi}.$$

With the modulus of γ_{12} set to maximum, the nullspace of the transition matrix (2.21) becomes two-dimensional and we obtain two steady-state solutions $\{\hat{\rho}_1, \hat{\rho}_2\}$. One of these steady states depends only on δ and φ and due to this non-interacting quality we call it a *dark state*:

$$\hat{\rho}_1 = \begin{bmatrix} \rho_{00} & \rho_{01} & \rho_{02} \\ \rho_{10} & \rho_{11} & \rho_{12} \\ \rho_{20} & \rho_{21} & \rho_{22} \end{bmatrix} = \frac{1}{2}\begin{bmatrix} 0 & 0 & 0 \\ 0 & 1-\delta & -\sqrt{1-\delta^2}e^{-i\varphi} \\ 0 & -\sqrt{1-\delta^2}e^{i\varphi} & 1+\delta \end{bmatrix}. \tag{4.1}$$

This state is pure, i.e. $\mathrm{tr}(\hat{\rho}_1^2) = 1$, and corresponds to the following superposition $|\phi\rangle$:

$$\hat{\rho}_1 = |\phi\rangle\langle\phi|, \qquad |\phi\rangle = \frac{e^{i\alpha}}{\sqrt{2}}\left(\sqrt{1-\delta}\,|1\rangle - \sqrt{1+\delta}e^{i\varphi}\,|2\rangle\right).$$

It follows that if the initial state $\hat{\rho}(0)$ can be partly decomposed into the dark state $|\phi\rangle\langle\phi|$ and some other state, the former part of the initial state remains constant. Furthermore, the expression for the general steady-state solution has a discontinuity at this point and the numerical calculations in the neighbourhood of this point need to be performed carefully. The second steady-state solution corresponds to a mixed state which is in thermodynamic equilibrium at temperature T,

$$\hat{\rho}_2 = \begin{bmatrix} \rho_{00} & \rho_{01} & \rho_{02} \\ \rho_{10} & \rho_{11} & \rho_{12} \\ \rho_{20} & \rho_{21} & \rho_{22} \end{bmatrix} = \frac{1}{1+3n}\begin{bmatrix} 1+n & 0 & 0 \\ 0 & n & 0 \\ 0 & 0 & n \end{bmatrix}. \tag{4.2}$$

4.2 Coherence parameters

We now proceed to the QHE and start by introducing a more convenient parametrization. The moduli of the dot product terms are bounded by the Cauchy-Schwartz inequality,

$$|\mathbf{d}_{b1}\cdot\mathbf{d}_{b2}^{*}|\leq|\mathbf{d}_{b1}|\,|\mathbf{d}_{b2}|\,,\qquad |\mathbf{d}_{\alpha1}\cdot\mathbf{d}_{\alpha2}^{*}|\leq|\mathbf{d}_{\alpha1}|\,|\mathbf{d}_{\alpha2}|\,.$$

Let us denote the phases of $\mathbf{d}_{b1}\cdot\mathbf{d}_{b2}^{*}$ and $\mathbf{d}_{\alpha1}\cdot\mathbf{d}_{\alpha2}^{*}$ as φ_h and φ_c respectively. To control the moduli of γ_{12c} and γ_{12h}, we introduce two real parameters t_h and t_c where $t_h, t_c\in\langle 0,1\rangle$,

$$\mathbf{d}_{b1}\cdot\mathbf{d}_{b2}^{*}=|\mathbf{d}_{b1}|\,|\mathbf{d}_{b2}|\,(1-t_h)e^{i\varphi_h},\qquad \mathbf{d}_{\alpha1}\cdot\mathbf{d}_{\alpha2}^{*}=|\mathbf{d}_{\alpha1}|\,|\mathbf{d}_{\alpha2}|\,(1-t_c)e^{i\varphi_c}.$$

We will refer to the case when the moduli are at maximum and when there is no decoherence, i.e. $\Lambda=t_h=t_c=0$, as the *maximum coherence* case. Next, we would like to control the ratios γ_{1c}/γ_{2c} and γ_{1h}/γ_{2h}, while keeping the sums $\gamma_{1c}+\gamma_{2c}$ and $\gamma_{1h}+\gamma_{2h}$ constant. To achieve this, we introduce two parameters δ_c and δ_h where $\delta_c,\delta_h\in\langle -1,1\rangle$:

$$\begin{aligned}
&\gamma_{1h}=\gamma_h(1+\delta_h), && \gamma_{1c}=\gamma_c(1+\delta_c), && \gamma_{12c}=\sqrt{\gamma_{1c}\gamma_{2c}}(1-t_c)e^{i\varphi_c},\\
&\gamma_{2h}=\gamma_h(1-\delta_h), && \gamma_{2c}=\gamma_c(1-\delta_c), && \gamma_{12h}=\sqrt{\gamma_{1h}\gamma_{2h}}(1-t_h)e^{i\varphi_h}.
\end{aligned}$$

We will refer to the cases $\delta_c=\delta_h$ and $\delta_c=-\delta_h$ as *same channel preference* and *opposite channel preference* respectively and to the case $\delta_c=\delta_h=0$ as the *no channel preference* case. Note that these cases then affect the use of the channels $(b\leftrightarrow 1\leftrightarrow\alpha)$ and $(b\leftrightarrow 2\leftrightarrow\alpha)$. With these definitions, the general steady state solution is determined by 14 real parameters,

$$\vec{\rho}_{st}=\vec{\rho}_{st}(n_c,n_h,N_c,\gamma_h,\gamma_c,\Gamma,\Gamma_c,\delta_h,\delta_c,\varphi_h,\varphi_c,t_h,t_c,\Lambda). \tag{4.3}$$

However, the populations can only depend on the relative phase between the dot products $\mathbf{d}_{b1}\cdot\mathbf{d}_{b2}^{*}$ and $\mathbf{d}_{\alpha1}\cdot\mathbf{d}_{\alpha2}^{*}$, i.e. between the rates γ_{12c} and γ_{12h}, which we denote θ:

$$\theta=|\varphi_h-\varphi_c|\,. \tag{4.4}$$

To study the effects of coherence, we will usually fix $\{n_c,n_h,N_c,\gamma_h,\gamma_c,\Gamma_c,\Gamma\}$ and vary the parameters of interest $\{\delta_h,\delta_c,\theta,t_h,t_c,\Lambda\}$ which we shall refer to as the *coherence parameters*. The significance of these parameters can be seen in fig. 4.1.

Figure 4.1: Four current-voltage characteristics obtained by variation of Γ, for model parameters B (see Appendix) in the maximum coherence case $\Lambda=t_h=t_c=0$.

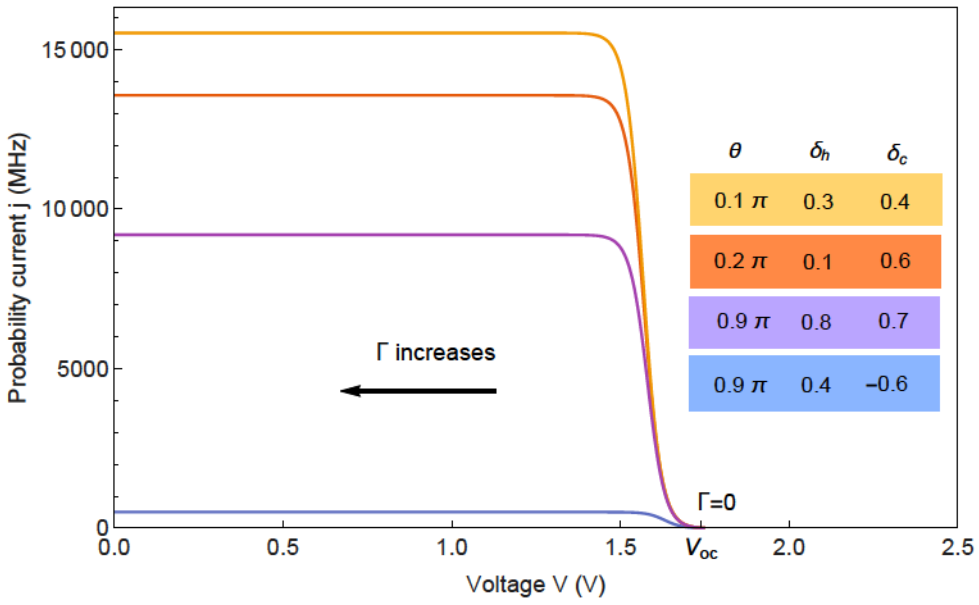

The figure 4.1 shows that while the overall behaviour of the current-voltage characteristics remains the same, the current can be significantly affected by these parameters (in this case by δ_h, δ_c and θ).

4.3 Dark state of the QHE

The QHE consists of two V-type systems and we find that for certain coherence parameters $\{\delta_h, \delta_c, \theta, t_h, t_c, \Lambda\}$ there exists a dark state of the whole QHE. The dark state emerges in the case of in-phase maximum coherence together with the same channel preference case, i.e. for $\theta = \Lambda = t_c = t_h = 0$ ($\varphi_h = \varphi_c = \varphi$) and $\delta_h = \delta_c = \delta$. The dark state then has the form:

$$|\phi\rangle = \frac{e^{i\alpha}}{\sqrt{2}}\left(\sqrt{1-\delta}\,|1\rangle - \sqrt{1+\delta}e^{i\varphi}\,|2\rangle\right),$$

$$\hat{\rho}_S = |\phi\rangle\langle\phi| = \begin{bmatrix} \rho_{bb} & \rho_{b1} & \rho_{b2} & \rho_{b\alpha} & \rho_{b\beta} \\ \rho_{1b} & \rho_{11} & \rho_{12} & \rho_{1\alpha} & \rho_{1\beta} \\ \rho_{2b} & \rho_{21} & \rho_{22} & \rho_{2\alpha} & \rho_{2\beta} \\ \rho_{\alpha b} & \rho_{\alpha 1} & \rho_{\alpha 2} & \rho_{\alpha\alpha} & \rho_{\alpha\beta} \\ \rho_{\beta b} & \rho_{\beta 1} & \rho_{\beta 2} & \rho_{\beta\alpha} & \rho_{\beta\beta} \end{bmatrix} = \frac{1}{2}\begin{bmatrix} 0 & 0 & 0 & 0 & 0 \\ 0 & 1-\delta & -\sqrt{1-\delta^2}e^{-i\varphi} & 0 & 0 \\ 0 & -\sqrt{1-\delta^2}e^{i\varphi} & 1+\delta & 0 & 0 \\ 0 & 0 & 0 & 0 & 0 \\ 0 & 0 & 0 & 0 & 0 \end{bmatrix}. \tag{4.5}$$

Note that the expression for the general steady-state solution has a discontinuity for these parameters accounting for the extra dimension (the null space of the transition matrix $\hat{M}$ is two-dimensional).

4.4 Analytically treatable parameter regime

To demonstrate the effects of coherence on a situation that is to a large extent treatable analytically, we adopt a parameter regime inspired by Dorfman et al. [8],

$$n_h \gg 1 \gg n_c \approx N_C, \qquad \gamma_c \ll \Gamma_c \ll \gamma_h \approx \Gamma. \tag{4.6}$$

Specifically, we introduce a scaling parameter ϵ so that:

$$\epsilon = N_C = n_c = n_h^{-1} = \frac{\gamma_c}{\Gamma_c} = \frac{\Gamma_c}{\gamma_h} = \frac{\Gamma_c}{\Gamma}. \tag{4.7}$$

This reduces the dependency of the populations from 13 model parameters to just 7:

$$\{n_c, n_h, N_c, \gamma_h, \gamma_c, \Gamma, \Gamma_c, \delta_h, \delta_c, t_h, t_c, \theta, \Lambda\} \to \{\epsilon, \delta_h, \delta_c, t_h, t_c, \theta, \Lambda\}.$$

Note that we replaced the absolute phases φ_c and φ_c with the relative phase θ since only the relative phase can affect the populations.

4.5 Classical current

We can find the current in the no coherence case, which we denote $\bar{j}$, by either setting the dot products of the transition dipole moments to zero ($t_h = t_c = 1$) or by increasing the decoherence constant Λ to infinity,

$$\bar{j} = \lim_{\Lambda\to\infty} j = j|_{t_h=t_c=1}. \qquad (j \overset{\text{s.s.}}{=} \Gamma\rho_{\alpha\alpha}) \tag{4.8}$$

The dependency of the steady-state populations on $\{\Lambda, \theta, t_h, t_c\}$ then vanishes and we find in the regime of sec. 4.4 that the current is proportional to the rate γ_c,

$$\bar{j}(\gamma_c, \epsilon, \delta_h, \delta_c) = \gamma_c \frac{2\left(\delta_h^2 - 1\right) + 2\epsilon\left(\delta_h^2 - 1\right) + 2\epsilon^3\left(\delta_c^2 - 1\right) + o(\epsilon^4)}{3\left(\delta_h^2 - 1\right) + 4\epsilon\left(\delta_h^2 - 1\right) + 2\epsilon^2\left(\delta_h^2 - 1\right) - 4\epsilon^3\left(3 + \delta_c\delta_h - 2\delta_h^2\right) + o(\epsilon^4)},$$

$$\bar{j} \xrightarrow{\epsilon \to 0} \gamma_c \frac{2}{3}. \tag{4.9}$$

Without coherence the current flows classically so that the channels $(b \leftrightarrow 1 \leftrightarrow \alpha)$ and $(b \leftrightarrow 2 \leftrightarrow \alpha)$ operate separately. We can verify this by varying the strengths of the rates γ_{1c}, γ_{2c} and γ_{1h}, γ_{2h} in the same channel preference case $(\delta_c = \delta_h = \delta)$ where the sum of the rates is constant,

$$\gamma_{1c} + \gamma_{2c} = \gamma_c(1 + \delta_c) + \gamma_c(1 - \delta_c) = 2\gamma_c,$$
$$\gamma_{1h} + \gamma_{2h} = \gamma_h(1 + \delta_h) + \gamma_h(1 - \delta_h) = 2\gamma_h.$$

Specifically, we find that the steady-state populations do not depend on δ and therefore the current remains constant. The extreme cases of same channel preference where $\delta_c = \delta_h = \pm 1$ correspond to the use of only one of the two channels.

On the other hand, in the extreme opposite channel preference case with $\delta_c = -\delta_h = 1$ which corresponds to $\gamma_{2c} = \gamma_{1h} = 0$, we effectively break both channels, i.e. $(b \not\leftrightarrow 1 \leftrightarrow \alpha)$ and $(b \leftrightarrow 2 \not\leftrightarrow \alpha)$. Therefore the current vanishes for $\delta_c = -\delta_h = \pm 1$,

$$\bar{j}|_{\delta_c = -\delta_h = \pm 1} = 0. \tag{4.10}$$

4.6 Coherent current

We now leave the no coherence case and look at the dependency of the steady-state current on the coherence parameters $\{\delta_h, \delta_c, \theta, t_h, t_c, \Lambda\}$. In the maximum coherence case, the most striking dependence is the dependence of the current on the relative phase θ, see fig. 4.2.

Figure 4.2: The steady-state probability current j in units of γ_c (Hz) vs the relative phase θ in the maximum coherence and no channel preference cases, shown for different values of the decoherence rate Λ (also in the units of γ_c). The other model parameters are determined by ϵ, see sec. 4.4.

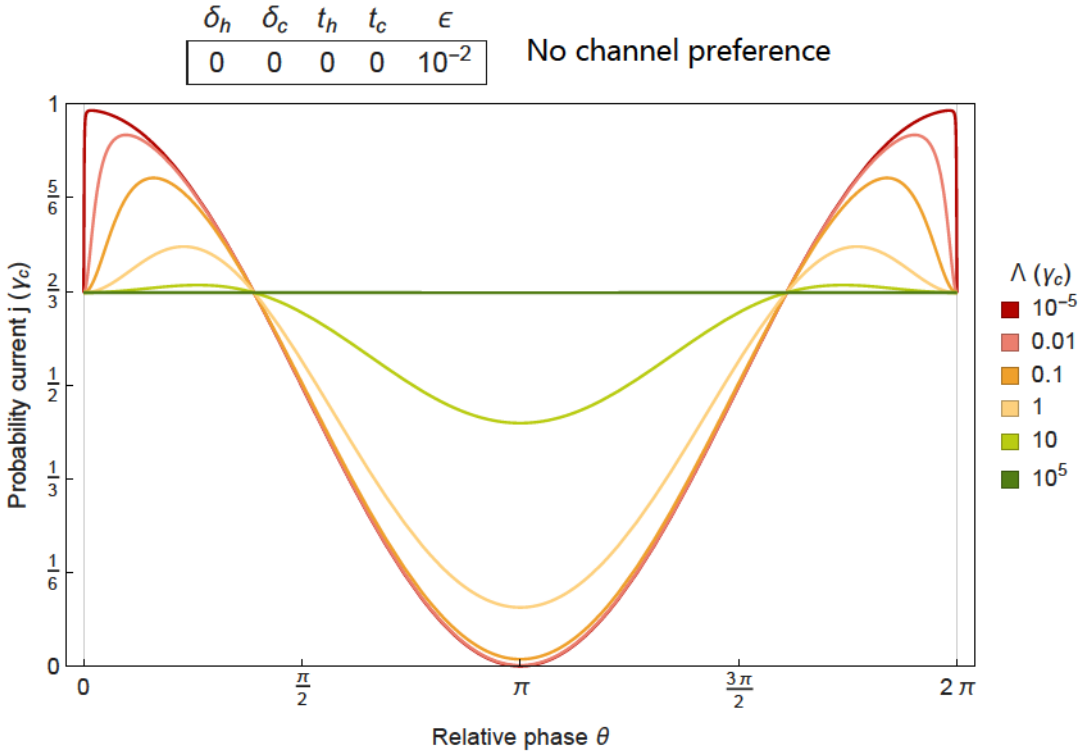

As we can see in fig. 4.2, for growing values of the decoherence rate Λ the behaviour of the current j approaches the classical current $\bar{j}$, i.e. it approaches the constant value $\bar{j}/\gamma_c \approx 2/3$. On the other hand, for smaller decoherence values the current becomes hindered when the coherence rates γ_{12h} and γ_{12c} are out of phase, $\theta \approx \pi + 2\pi k$, $k \in Z$, and enhanced when they are in phase, $\theta \approx 2\pi k$, $k \in Z$. Without decoherence, the current resembles an interference pattern and is roughly proportional to $\cos^2(\theta/2)$.

Furthermore, we notice that as we approach small values of decoherence (red), the current is forming a discontinuity at $\theta = 2\pi k$, $k \in Z$. This is consistent with the presence of the singularity for this value in the general steady-state solution, accounting for the dark state of the QHE. The singularity occurs for the line $\theta = \Lambda = t_c = t_h = 0$, $\delta_h = \delta_c = \delta$ and we find that the limiting value of the current j varies with the path of approach to it.

For example, two different sequences of limits yield:

$$j'(\theta, t_h, \gamma_c, \epsilon) = \lim_{t_c\to 0}\lim_{\delta_h\to\delta}\lim_{\delta_c\to\delta}\lim_{\Lambda\to 0} j,$$

$$\lim_{t_h\to 0}\lim_{\theta\to 0} j' = \gamma_c \frac{1+\epsilon}{1+2\epsilon+\epsilon^2+5\epsilon^3+3\epsilon^4} \xrightarrow{\epsilon\to 0} \gamma_c, \tag{4.11}$$

$$\lim_{\theta\to 0}\lim_{t_h\to 0} j' = \gamma_c \frac{2(1+\epsilon)}{3+4\epsilon+2\epsilon^2+10\epsilon^3+6\epsilon^4} \xrightarrow{\epsilon\to 0} \gamma_c \frac{2}{3}. \tag{4.12}$$

Let us now consider the case where $\gamma_{1c} \neq \gamma_{2c}$ and $\gamma_{1h} \neq \gamma_{2h}$. The figure 4.3 shows two cases of same channel preference corresponding to the rates γ_{1c} and γ_{1h} being 3 times and then 19 times stronger than the rates γ_{2c} and γ_{2h} respectively.

Figure 4.3: The steady-state probability current j vs the relative phase θ in same channel preference cases corresponding to 3-fold and 19-fold relative channel strength.

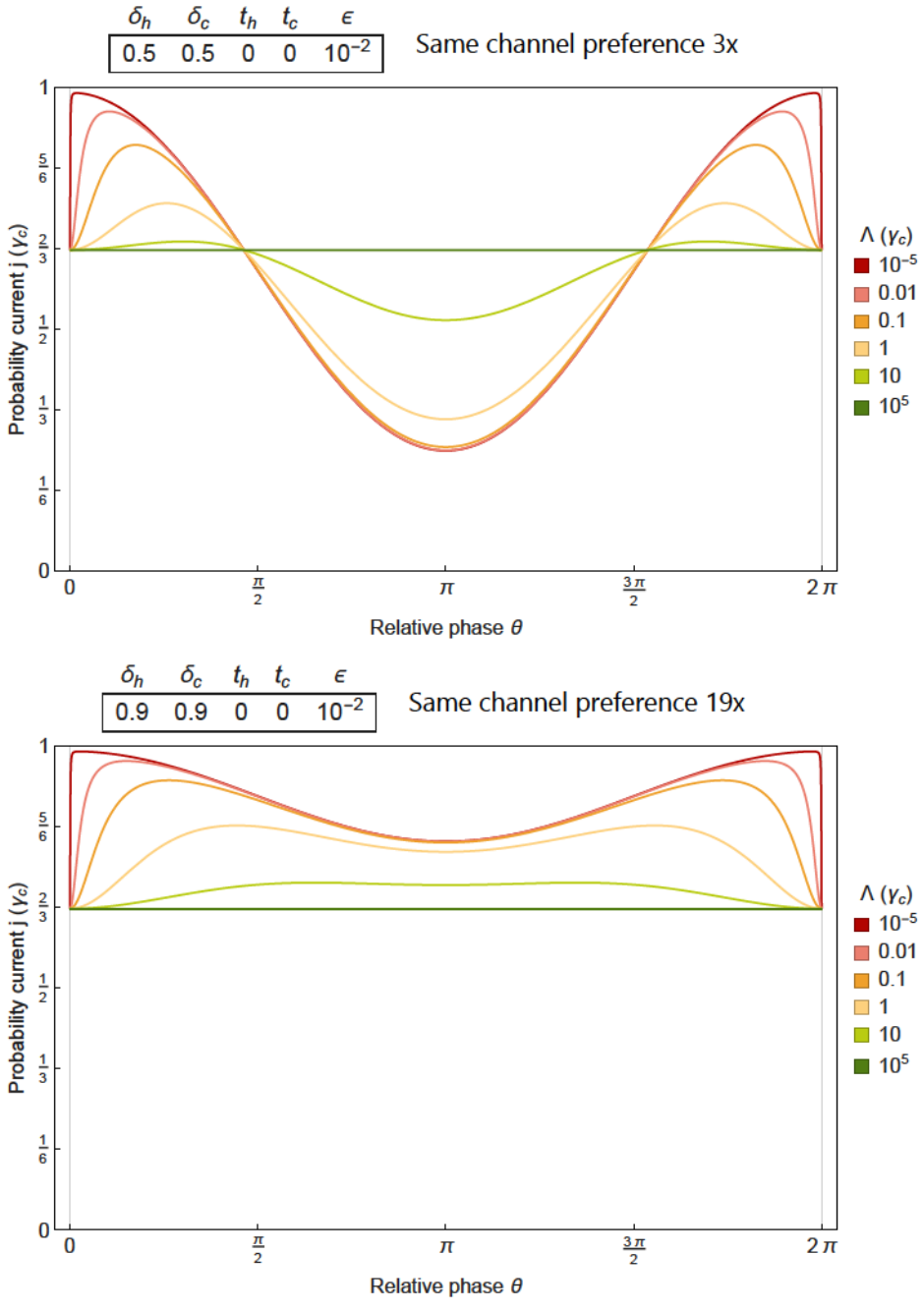

We still observe the formation of the discontinuity when exactly in phase, $\theta = 2\pi k$, $k \in Z$. However, we find that the current no longer vanishes for $\theta = \pi + 2\pi k$, $k \in Z$ and as δ approaches ± 1 ($\delta = \delta_c = \delta_h$), the current approaches the maximum value of the no channel preference case.

If we compare this with the opposite channel preference case in fig. 4.4, complete destructive interference is still present here and the current is overall diminished. We also no longer observe the discontinuous behaviour at $\theta = 2\pi k$, $k \in Z$ because we have moved away from the conditions of the dark state ($\theta = \Lambda = t_c = t_h = 0$ and $\delta_h = \delta_c = \delta$) which require same channel preference.

Figure 4.4: The steady-state probability current j vs the relative phase θ in two opposite channel preference cases corresponding to 3-fold and 19-fold relative channel strength.

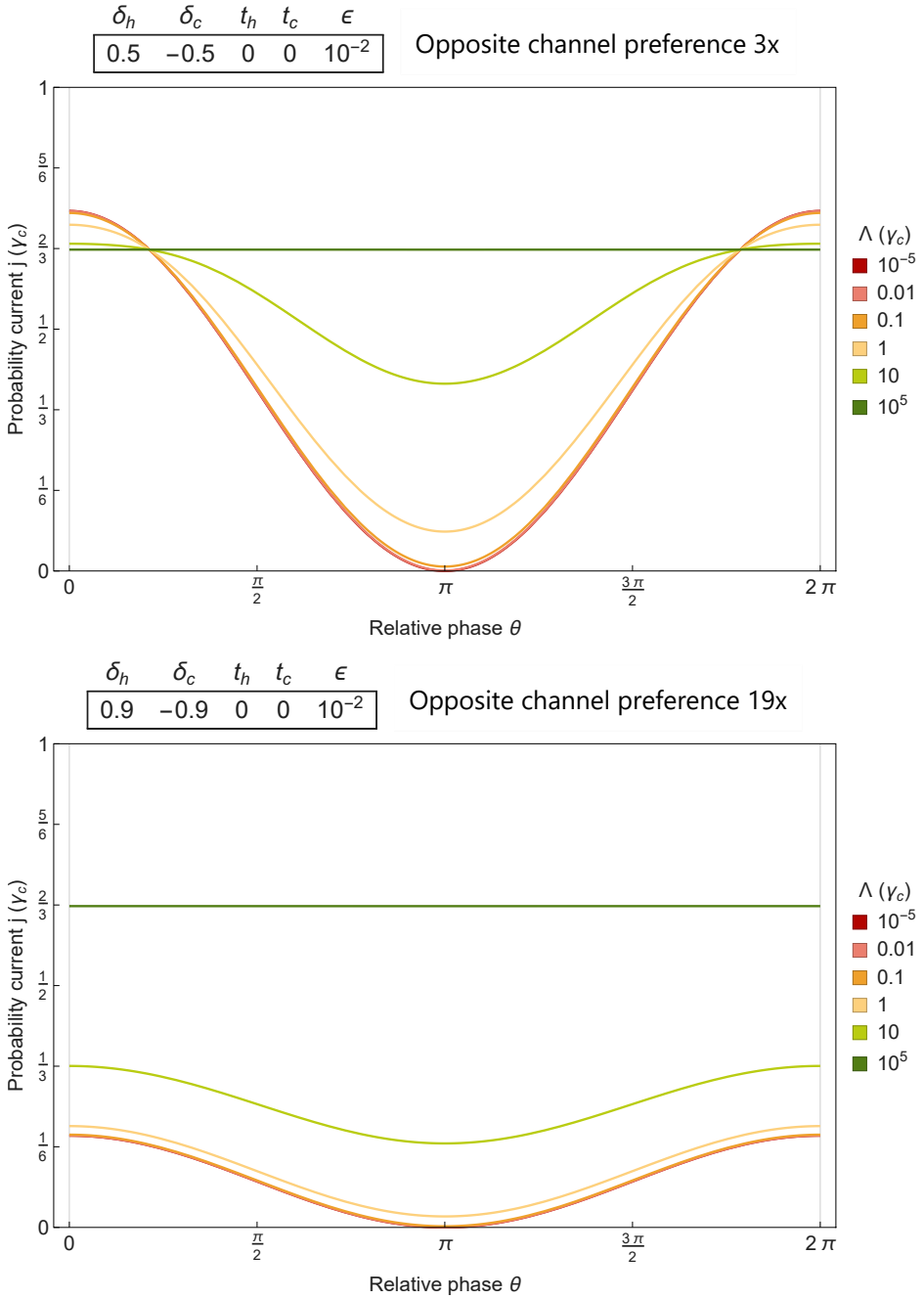

Let us take a look at the dependence of the destructive interference ($\theta = \pi$) on the parameters δ_h and δ_c, see fig. 4.5 (note that we omit the extreme cases where $\delta_h = \pm 1$ and $\delta_c = \pm 1$).

Figure 4.5: Contour plot of the dependence of the steady-state probability current j on δ_h and δ_c at maximum coherence and with the rates γ_{12c} and γ_{12h} out of phase ($\theta = \pi$).

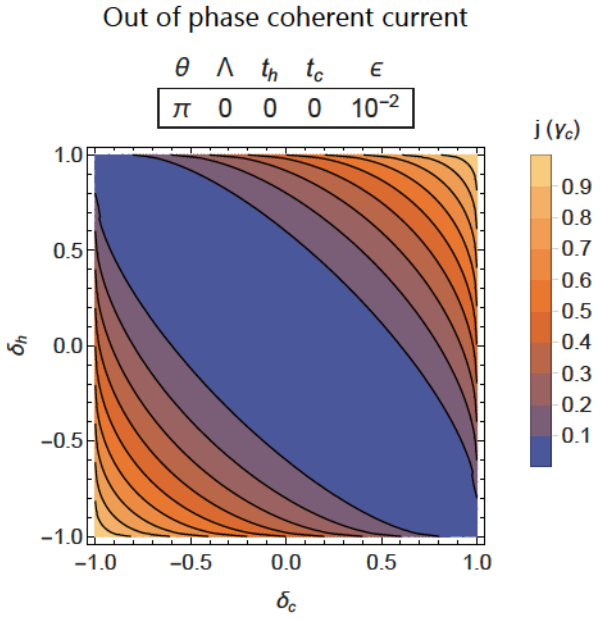

We see that the destructive interference is significant when we are near the case of opposite channel preference $\delta_h = -\delta_c$, and it is diminished with strong same channel preference $\delta_h = \delta_c$.

Interestingly, if we turn off the rate Γ in the case of out of phase, maximum coherence and opposite channel preference (i.e. $\Lambda = t_h = t_c = 0$, $\delta_h = -\delta_c$, $\theta = \pi$, $\Gamma = 0$), we obtain a two-dimensional steady-state solution space spanned by the following unnormalized states $\hat{Q}_1$ and $\hat{Q}_2$:

$$\hat{Q}_1 = \begin{bmatrix} 0 & 0 & 0 & 0 & 0 \\ 0 & n_c(1-\delta_h)/2 & -n_c\sqrt{1-\delta_h^2}e^{-i\varphi_h}/2 & 0 & 0 \\ 0 & -n_c\sqrt{1-\delta_h^2}e^{i\varphi_h}/2 & n_c(1+\delta_h)/2 & 0 & 0 \\ 0 & 0 & 0 & n_c+1 & 0 \\ 0 & 0 & 0 & 0 & 0 \end{bmatrix},$$

$$\hat{Q}_2 = \begin{bmatrix} n_c(1+N_c)(1+n_h) & 0 & 0 & 0 & 0 \\ 0 & n_c(1+N_c)n_h & 0 & 0 & 0 \\ 0 & 0 & n_c(1+N_c)n_h & 0 & 0 \\ 0 & 0 & 0 & (1+n_c)(1+N_c)n_h & 0 \\ 0 & 0 & 0 & 0 & n_cN_c(1+n_h) \end{bmatrix}.$$

While the unnormalized state $\hat{Q}_2$ corresponds to the classical steady state ($\gamma_{12c} = \gamma_{12h} = 0$) with the transition $\{\alpha, \beta\}$ turned off ($\Gamma = 0$), we notice that $\hat{Q}_1$ does not populate the two lowest energy levels. When we turn the transition $\{\alpha, \beta\}$ on, i.e. $\Gamma > 0$, the resulting

steady-state solution (there is only one now) corresponds to the combination of these two with the lowest possible energy:

$$\hat{\rho}_S = A(\hat{Q}_2 - (1 + N_c)n_h\hat{Q}_1), \tag{4.13}$$

where A is a normalization constant. To see this, we examine the unnormalized states $\hat{Q}_1$ and $\hat{Q}_2$ and the eq. (4.13). The term $-(1+N_c)n_h\hat{Q}_1$ removes (from the state $\hat{Q}_2$) the largest amount of probability from the upper states while keeping the populations non-negative and thus, indeed, yields the lowest possible energy of the open system. The population $\rho_{\alpha\alpha}$ is then zero which is consistent with the vanishing of the steady-state current $j = \Gamma\rho_{\alpha\alpha}$ for Γ positive.

Lastly, let us look at the dependence of coherence effects on the parameters t_c and t_h which control the moduli of γ_{12h} and γ_{12c}, see fig. 4.6. We find that the expression for the general steady-state solution is not symmetric (with respect to t_h and t_c) and within our parameter regime (sec. 4.4), near-perfect alignment is required for strong effects of coherence (i.e. t_c and t_h very close to zero).

Figure 4.6: Two contour plots of the dependence of the steady-state current j on the parameters t_c and t_h, controling the moduli of γ_{12c} and γ_{12h} resp. Both plots correspond to out of phase, no channel preference case, and two values of ϵ which controls the other model parameters.

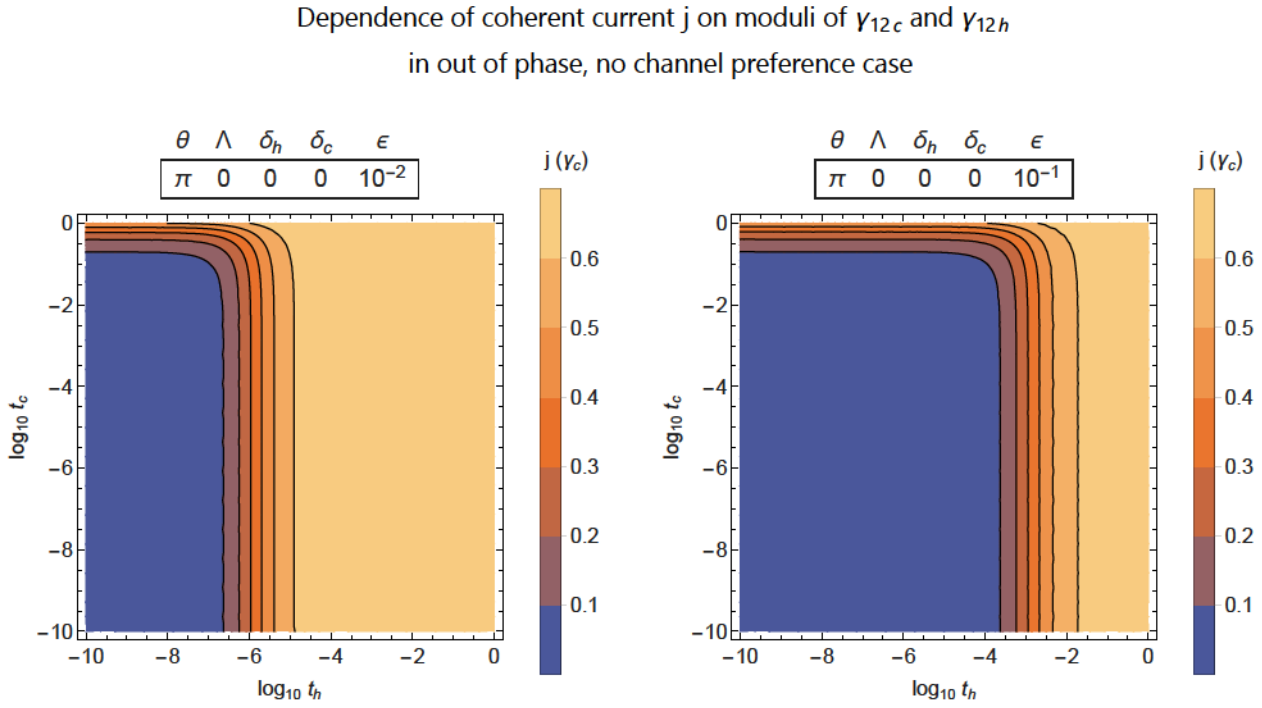

4.7 Current enhancement

So far, we have only shown the enhancement and reduction of current for the parameter regime in sec. 4.4. However, for the assumed typical energy spacings (see Appendix), the assumption that $n_h \gg 1$ is inconsistent with the hot bath temperature 6000 K and corresponds to temperatures above 10^6 K. The following figure 4.7 follows our parameter regime but adjusts the occupation number n_h by using the temperature 6000 K.

Figure 4.7: Steady state probability current j in units of γ_c (Hz) vs the relative phase θ in the maximum coherence and no channel preference cases, shown for different values of the decoherence rate Λ (also in the units of γ_c).

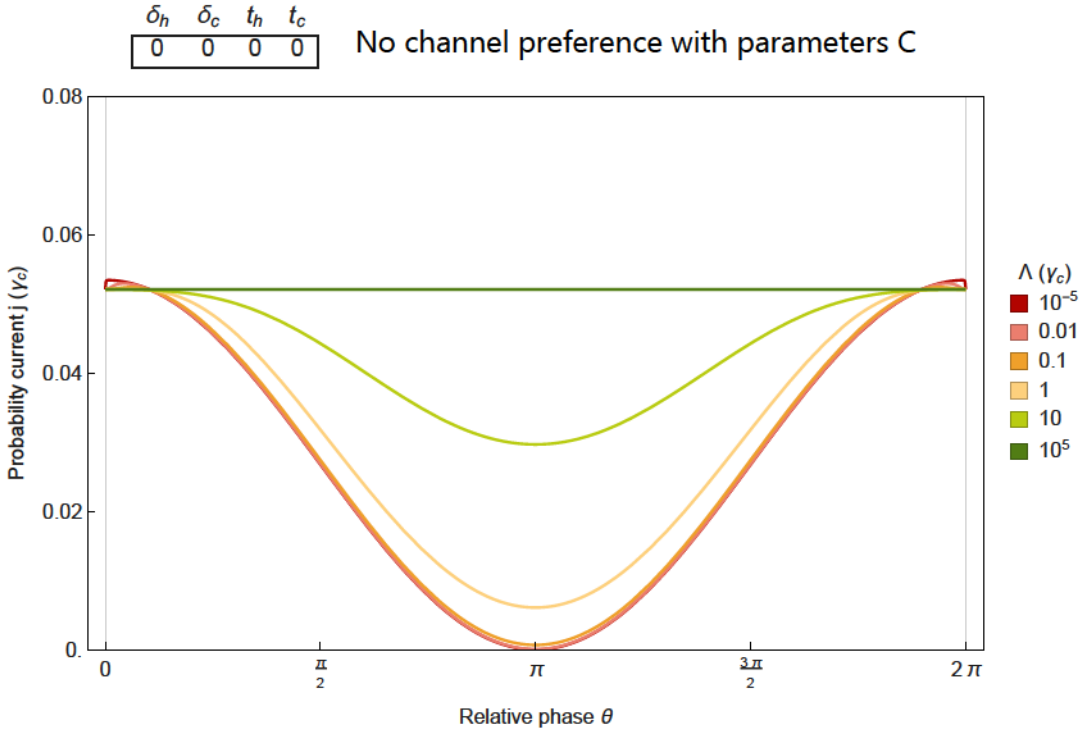

We see that regions of the relative phase where the current is enhanced above the classical value have diminished (as opposed to fig. 4.2) and the current is only lowered due to destructive interference. Furthermore, we find that same channel preference only removes the destructive interference and the current does not exceed the maximum value of the no channel preference case.

Summary

A standard Markovian QOME of the Lindblad form was used to explore the effects of coherence in a simple QHE model with two degenerate upper levels. The QOME works with a quantized electromagnetic field, two heat baths at different temperatures and uses the dipole and weak-coupling approximations resulting in the neglection of Lamb and Stark shift terms. The QHE model was inspired by previous work of Dorfman et al. [8] and mimics the photosynthetic cycle of two donor molecules and one acceptor molecule at the heart of the reaction center.

The QHE exhibits a current-voltage characteristic of a solar cell with an efficiency that is proportional to the voltage and approaches the Carnot limit for small currents. For voltages near the open circuit voltage, the power output is roughly proportional to the current and therefore enhancement of the current results in equal enhancement of the power output.

The behavior of coherences is affected by two complex terms. These correspond to the dot products of two pairs of the transition dipole moments governing the transitions to the upper degenerate levels. Whereas near perfect alignment is necessary for significant effects of coherence on the steady-state current, without the alignment, the current behaves classically. In the maximum coherence case, the current is highly dependent on the relative phase between these two terms and it vanishes when they are out of phase, strongly resembling destructive interference.

Enhancement of the current above the classical value was predicted for small relative phases, in a parameter regime inspired by Dorfman et al. [8]. However, this parameter regime assumes a large photon occupation number corresponding to the increase of the temperature of the hot bath from 6000 K to an extreme temperature of the order 10^6 K. Without this boost of temperature, we predict only destructive interference lowering the current.

Finally, we note that all programs used for the computation of the presented results have been previously checked to produce normalized solutions which converge to the Gibbs distribution for equal bath temperatures and the rate Γ set to zero.

Appendix

Example parameters

In order to illustrate features of the QHE, we use model parameters inspired by Dorfman et al. [8] (see the table 5.1 below).

Table 5.1: Used example model parameters

	$E_{12}-E_b$	$E_{12}-E_\alpha$	$E_\beta-E_b$	Γ_c	γ_c	γ_h	Γ	δ_h	δ_c	T_c	T_h
	cm^{-1}	cm^{-1}	cm^{-1}	cm^{-1}	cm^{-1}	cm^{-1}	cm^{-1}	cm^{-1}	cm^{-1}	K	K
A	14856	1611	1611	300	100	0.01	-	0	0	300	6000
B	14856	1611	1611	70	10	300	-	-	-	300	6000
C	14856	1611	1611	300	20	700	700	0	0	300	6000
D	14856	1611	1611	100	100	20	0.001	0	0	12000	12000

Time evolution

The figures 5.8 and 5.9 show the time evolution of the following initial state:

$$\hat{\rho}_S(0) = |\phi\rangle\langle\phi|, \qquad |\phi\rangle = \frac{e^{i\alpha}}{\sqrt{2}}\left(\sqrt{1-\delta}\,|1\rangle - \sqrt{1+\delta}e^{i\varphi}\,|2\rangle\right), \tag{5.14}$$

and illustrate the fact that a small pertubation in the dark state conditions causes significant change in the resulting steady state.

Figure 5.8: The evolution of $\hat{\rho}_S(0)$ (eq. 5.14) with $\varphi = 0$, under conditions where this state corresponds to the dark state (a steady state). These conditions are maximum, in phase coherence and same channel preference: $\theta = \Lambda = t_c = t_h = 0$, $\delta_h = \delta_c = \delta$ and $\varphi_c = \varphi_h = \varphi$. The element ρ_{re} corresponds to the real part of ρ_{12} and the imaginary part is zero.

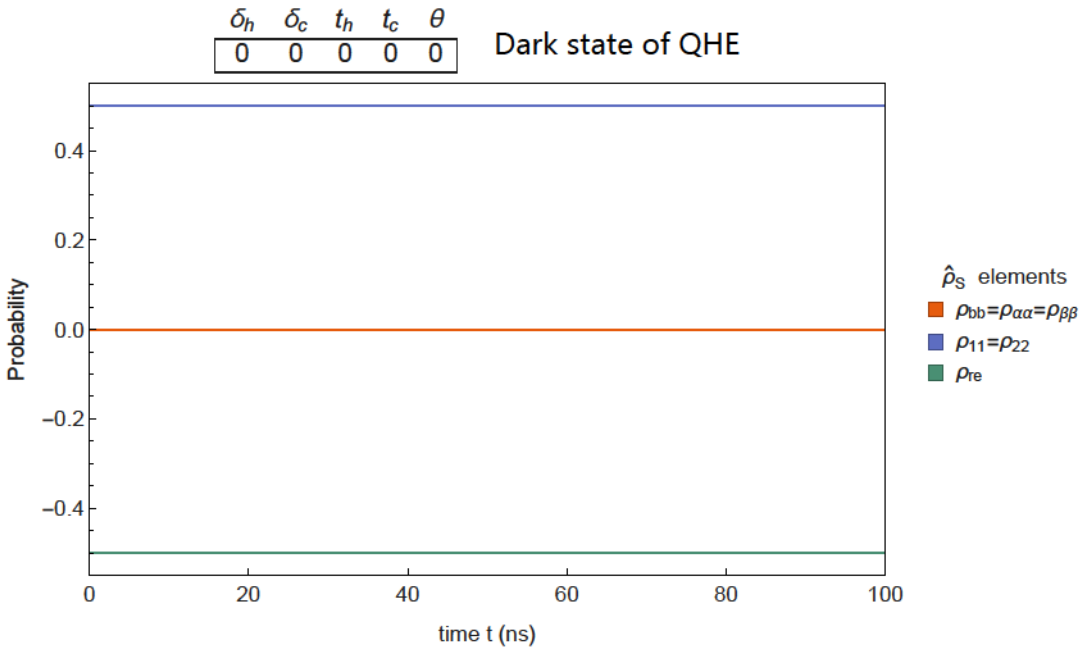

Figure 5.9: The evolution of $\hat{\rho}_S(0)$ (eq. 5.14) with $\varphi = 0$, under conditions deviating from the dark state conditions such that $t_h = t_c \neq 0$. The element ρ_{re} corresponds to the real part of ρ_{12} and the imaginary part is zero. The dashed lines represent the steady-state values.

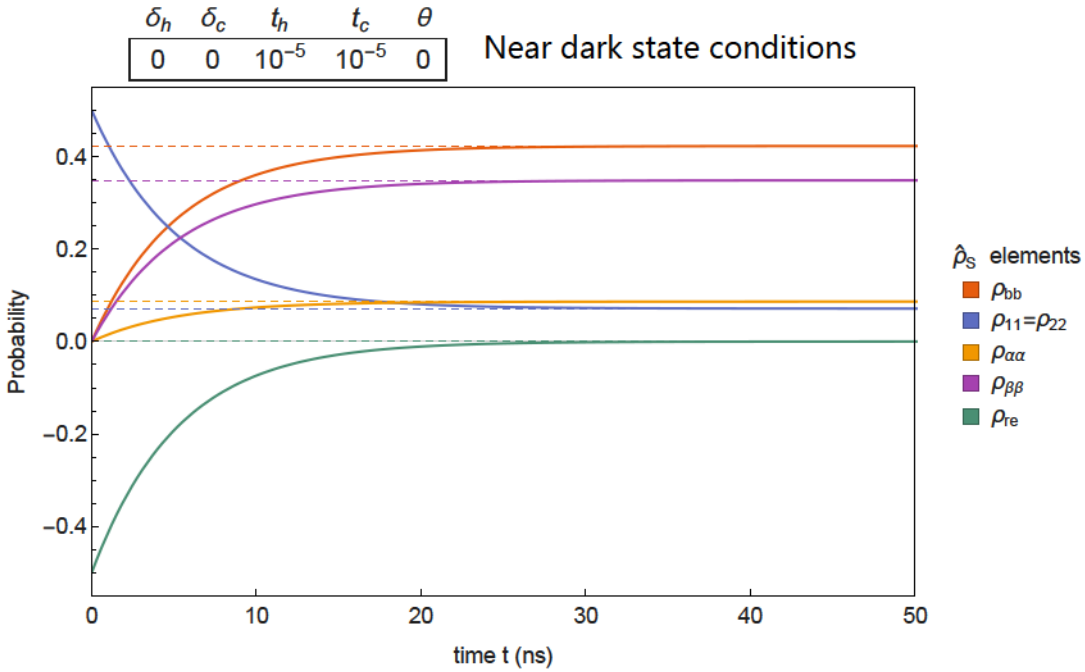

Bibliography

[1] Alexander Streltsov, Gerardo Adesso, Martin B. Plenio, *Quantum Coherence as a Resource*. Rev. Mod. Phys. 89, 041003. (2017)

[2] G. S. Engel, T. R. Calhoun, E. L. Read, T. K. Ahn, T. Mančal, Y. C. Cheng, R. E. Blankenship, and G. R. Fleming, *Evidence for wavelike energy transfer through quantum coherence in photosynthetic systems*. Nature 446, p. 782–786. (2007)

[3] M. Sarovar, A. Ishizaki, G. R. Fleming, K. B. Whaley, *Quantum entanglement in photosynthetic light harvesting complexes*. Nature Physics, 6, p. 462–467. (2010)

[4] A. Vaziri, M.B. Plenio, *Quantum coherence in ion channels: Resonances, Transport and Verification*. New J. Phys. 12, 085001. (2010)

[5] Don Devault, Britton Chance, *Temperature Dependence of Cytochrome Oxidation Rate in Chromatium. Evidence for Tunneling.* Biophys J. 6(6), p. 825–847. (1966)

[6] Stephan Hoyer, Akihito Ishizaki, K. Birgitta Whaley, *Spatial propagation of excitonic coherence enables ratcheted energy transfer.* Phys. Rev. E 86, 041911 (2012)

[7] R. E. Blankenship, *Molecular Mechanisms of Photosynthesis*. Blackwell Science Ltd. (2008)

[8] Konstantin E. Dorfman, Dmitri V. Voronine, Shaul Mukamel, Marlan O. Scully, *Photosynthetic reaction center as a quantum heat engine*. PNAS U.S.A. vol. 110 no. 8, p. 2746–2751. (2013)

[9] Heinz-Peter Breuer, Francesco Petruccione, *The Theory of Open Quantum Systems*. Oxford University Press, New York. (2002)

[10] Ramamurti Shankar, *Principles of Quantum Mechanics*. Springer, New York. (2014)

[11] Paola Cappellaro, MIT lecture notes. *Quantum Theory of Radiation Interactions*. Chapter 8. (Fall 2012)

`https://ocw.mit.edu/courses/nuclear-engineering/22-51-quantum-theory-of-radiation-interactions-fall-2012/lecture-notes/MIT22_51F12_Notes.pdf`

[12] Christian Majenz, Tameem Albash, Heinz-Peter Breuer, Daniel A. Lidar, *Coarse-Graining Can Beat the Rotating Wave Approximation in Quantum Markovian Master Equations.* Phys. Rev. A 88, 012103. (2013)

[13] K. Kraus, *States, Effects and Operations, Fundamental Notions of Quantum Theory.* Springer-Verlag Berlin Heidelberg. (1983)

[14] C. Creatore, M. A. Parker, S. Emmott, A. W. Chin, *An efficient biologically-inspired photocell enhanced by quantum coherence.* Phys. Rev. Lett. 111, 253601. (2013)

[15] M. O. Scully, M. S. Zubairy, *Quantum Optics*. Cambridge University Press. (2008)

[16] Marc Eichhorn, *Laser Physics: From Principles to Practical Work in the Lab*. Chapter 1. Springer, New York. (2014)

[17] Anatoly A. Svidzinsky, Konstantin E. Dorfman, Marlan O. Scully, *Enhancing photocell power by noise-induced coherence*. Coherent Optical Phenomena, vol. 1, p. 7–24. (2012)

[18] Chetan Singh Solanki, Hemant Kumar Singh, *Anti-reflection and Light Trapping in c-Si Solar Cells.* Section 2.4.2. Springer, New York. (2017)